Local and Global Baroclinic Instability of Zonally Varying Flow

R. T. PIERREHUMBERT

Geophysical Fluid Dynamics Laboratory/NOAA, Princeton, NJ 08542

(Manuscript received 3 January 1984, in final form 3 May 1984)

ABSTRACT

The baroclinic instability characteristics of zonally inhomogeneous basic states are examined with the intent of clarifying the factors governing the regional distribution of cyclogenesis. The vertical shear of the basic state wind is allowed to vary gradually in the zonal direction, so as to permit the representation of zonally localized regions of high baroclinicity. The resulting eigenvalue problem is solved directly by numerical means and also analytically via a WKB analysis. It was established that flows with localized baroclinicity can support two distinct classes of unstable modes, which we call "local" and "global." The local modes have peak amplitude downstream of the point of maximum baroclinicity, decay to zero exponentially upstream and downstream of the peak and do not require zonally periodic boundary conditions for their existence. The growth rate of a local mode is equal to the absolute growth rate (in the sense of Merkine) determined locally at the point of maximum shear. The absolute growth rate decreases when the vertically averaged zonal wind is increased, in contrast with the conventional locally determined maximum growth rate. Further properties of the local modes are discussed. The global modes, on the other hand, require periodic boundary conditions for their existence and have growth rates which are sensitive to the average baroclinicity over the domain. Global modes take a much longer time than local modes to emerge from random initial conditions.

On the basis of these results, it is suggested that the locally determined absolute growth rate is a useful diagnostic for assessing the stability properties of inhomogeneous flow. In this connection, a tentative analysis of the results of Frederiksen on planetary wave instabilities was found to be encouraging. Although only a simple model of baroclinic instability was considered in the present work, the techniques developed can be generalized to any kind of instability provided that there is a separation in spatial scale between the eddies and the basic state. It is thus proposed that there is a general link between absolute instability and the instability of nonparallel flow.

1. Introduction

The delineation of the factors governing the geographical distribution of cyclone occurrence is essential to the understanding of a number of other atmospheric phenomena of great importance. In the domain of long-range weather forecasting, for example, it is necessary to link the shifts in the storm tracks (which determine much of the anomalous weather) to shifts in the large-scale planetary wave pattern. Indeed, the positions of the storm tracks and their associated eddy fluxes of heat and vorticity may influence the state of the planetary waves themselves (Hoskins *et al.*, 1983). Inhomogeneous eddy fluxes arising from synoptic scale transients have also been implicated in the maintenance of blocking patterns (Green, 1977; Illari and Marshall, 1983). In connection with the latter, the distribution of cyclones relative to regions of high and low baroclinicity is particularly important. Even a cursory examination of the literature would reveal many other studies in which it was necessary to deal with the regional character of cyclogenesis.

The earth's atmosphere is characterized by localized regions of high baroclinicity, and therein lies the main difficulty: most of our understanding of cyclogenesis descends from studies of the instability of zonally homogeneous parallel flows. A fruitful attack on the problem of regional cyclogenesis has been developed in a series of papers by Frederiksen, in which the stability characteristics of stationary zonally varying flows were numerically determined (see Frederiksen, 1983 and references therein). Niehaus (1980, 1981) has pursued a parallel line of investigation for the problem of instability of forced waves in the Eady problem. In Frederiksen (1983) considerable agreement was found between the observed geographical distribution of synoptic scale eddy heat flux and the distribution predicted by the most unstable modes of the linear, zonally inhomogeneous stability problem. Nevertheless, in trying to understand the results of the stability calculation, one encounters a host of theoretical issues which have not yet been addressed.

Notably, the January Northern Hemisphere flow considered in Frederiksen (1983) yielded localized Pacific and Atlantic storm tracks, whereas the July pattern yielded a single unstable wave train which extended almost around the globe. Similarly, the idealized flow treated in Frederiksen (1979) yielded a

single weakly modulated wave train rather than localized storm tracks. What feature of the basic-state flow determines the degree of zonal localization? What is the physical mechanism responsible for the localization? What can be said about the effects of nonlinearity on the local character of the modes? The maximum amplitude of the mode is generally found *downstream* of the region of highest baroclinicity. Why is this the case? What determines how far downstream the maximum amplitude occurs? The most unstable mode for the January flow consists of an isolated Atlantic storm track, whereas the Pacific storm track appears only in a mode that exhibits an accompanying Atlantic storm track. Does this mean that cyclogenesis in the Pacific should in some way be correlated with cyclogenesis in the Atlantic? Finally, the growth rate of the most unstable mode found in Frederiksen (1979) was essentially unaffected by the presence of the idealized planetary wave, in contrast with the results on the effects of realistic waves reported in Frederiksen (1983). Can we derive a quantity that provides an *a priori* estimate of the degree of instability of such nonzonal flows?

The separation in spatial scale between stationary waves and the rapid instabilities that are found to develop on them suggests that the above issues can be approached through the consideration of some suitable local characteristics of the nonzonal basic-state flow. Specifically, one can define a local dispersion relation at each longitude by solving the stability problem relating complex frequency to zonal wavenumber as if the zonal flow at that particular longitude were extended uniformly around the globe. Under the assumption of slow zonal variation of the basic state, it would then be expected that the local dispersion relations would contain all the information necessary to determine the stability of the nonzonal state and the structure of the eigenmodes. But what property of the local dispersion relation characterizes the degree of instability of the nonzonal state and the degree of localization of the unstable modes? A reasonable first guess would be the growth rate of the fastest growing normal mode associated with each local dispersion relation, which can be generally measured by the local degree of supercriticality of the flow. In the case of two-layer flow without horizontal shear, for example, the Phillips criterion states that instability occurs only when the vertical shear exceeds a certain critical value; in this case, the amount by which the shear at each longitude exceeds the critical shear would seem to be of obvious importance. Indeed, Frederiksen (1978, 1980) attempted to relate the stability characteristics of idealized planetary waves to the pattern of zonal variation of supercriticality, making use of a heuristic generalization of the Phillips criterion that incorporated some of the effects of meridional shear. He established through numerical experimentation that the eigenmodes attain maximum amplitude downstream of the regions of maximum supercriticality, and that the amplitude of modulation of the unstable wave train increases with increasing zonal range of supercriticality. However, no attempt was made to explain these relationships analytically or physically. Moreover, no quantitative relation between the maximum supercriticality and the growth rate of the instability was found.

Further reflection reveals a serious problem with the use of local supercriticality as a guide to the stability characteristics of nonparallel flow. When a flow is zonally inhomogeneous, a wave packet has the possibility of propagating out of an unstable region before it has time to grow significantly; thus, the degree of instability of the flow should be sensitive to the joint effects of local propagation speed and local growth rate. The Phillips criterion, like other measures of the magnitude of local energy sources, manifestly fails in this regard, as it is insensitive to the addition of a mean flow.[1] The importance of propagation may also be arrived at through consideration of the symmetry properties of the basic flow. Consider, for example, synoptic scale quasi-geostrophic flow on the baroclinic beta-plane. In this system, the stability problem for parallel flow is invariant under the Galilean group, that is, the addition of constant zonal flow shifts the real parts of the eigenvalues of the problem by a corresponding amount without affecting the growth rates. If zonal inhomogeneity of the basic state is introduced, though, the Galilean invariance is broken, and the addition of a constant zonal flow can have a nontrivial effect. The fact that a wave packet can propagate out of an unstable region is central to the understanding of the instability of nonparallel flow. An analytical clarification of the role of the phenomenon is therefore essential.

Fortunately, a convenient mathematical apparatus is available for the analysis of the balance between propagation and growth of unstable wave packets. The answer lies in the concept of "absolute" versus "convective"[2] instability, which was introduced into

---

[1] In a spherical geometry, the addition of a barotropic flow to the basic state has two effects that cannot be isolated from each other. First, the flow alters the speed of propagation of wave packets. In addition, the meridional shear of the flow can stabilize or destabilize the perturbations. On a beta-plane, we can eliminate the latter effect by choosing a y-independent flow. On a sphere, the closest analog to such a flow is uniform super-rotation. The addition of such a flow changes the stability characteristics by changing the basic state vorticity gradient, entirely apart from its effects on wave propagation. The generalized Phillip criterion discussed in Frederiksen (1980) reflects only the vorticity gradient effect.

[2] The unfortunate term "convective" was introduced by investigators in the area of plasma physics, in which there is little risk of confusion of the phenomenon with the thermally driven convection familiar to fluid dynamicists. The term refers to wave packet propagation rather than any sort of thermally driven instability. As such, the terminology "advective" would be more congenial, though the original nomenclature is rather entrenched.

geophysical fluid dynamics by Merkine (1977). By way of illustration, consider the evolution of an initially localized disturbance in an unstable system that is infinite in the zonal (x) direction. The wave packet set up by the disturbance will grow, spread and propagate, but not all parts of the wave packet grow at the same rate. Consequently, we can distinguish between the "absolute" growth rate, corresponding to the growth rate at a fixed point x after a very long time has passed, and the "peak" growth rate, corresponding to the growth rate observed by following along with the moving peak of the wave packet. The latter is given by the most unstable normal mode, and the absolute growth rate will always be less than this value. Simply put, the absolute growth rate is the growth rate of the part of the wave packet that is left behind after the peak moves away. The absolute growth rate can be zero even when the peak growth rate is substantial, a situation known as "convective instability." The converse situation, in which the absolute growth rate is nonzero, is known as "absolute instability."

In connection with the zonally inhomogeneous stability problem, we wish to use the absolute instability concept to differentiate "local" modes from "global" modes. The former correspond to modes that grow *in situ* after the transient pulse has moved out of the unstable zone, while the latter arise in a cyclic domain when a wave packet passes repetitively through the same unstable zone, acquiring more energy on each pass. Given that real cyclones mature and decay before completing even a single circuit of the globe, we believe the latter class of modes to be nonphysical, in the sense that a given global mode is unlikely to appear by itself. Of course, the global modes may still be physical in the sense that a large number of them could be superposed in order to represent the transient evolution of a wave packet. It is our hypothesis that the local modes, when they exist, are characterized by the maximum *absolute* growth rate obtaining around the globe.

The connection between absolute instability and the instability of zonally inhomogeneous flow is the central theme of this paper. The structure of the unstable eigenmodes will be seen to arise naturally from this link. As the vehicle for exploring the theoretical issues raised above, we make use of an idealized model describing the baroclinic instability of a zonally varying two-layer flow on the beta-plane. This model is described in Section 2. In Section 3 we review the salient features of the theory of absolute instability of zonal flow and in Section 4 we present the results of a numerical computation of the most unstable eigenmodes for a family of zonally inhomogeneous basic states. These results clearly establish the quantitative link between absolute instability and local instability of nonparallel flow. This link is put on firm analytical footing through an asymptotic analysis of the problem via WKB techniques in Section 5. The requirements for localization and the reason the modes attain maximum amplitude downstream of the baroclinic zone are explained there as well. The general implications of our results are discussed in Section 6, and the most important conclusions are summarized in Section 7.

Gent and Leach (1976) and Niehaus (1981) performed illuminating WKB analyses of the instability of zonally varying flows. However, by neglecting the possibility of WKB "turning points" associated with absolute instability, these authors were able to find only global modes (in our terminology). The WKB analysis of the global modes in the two-layer model which we discuss briefly in Section 5c does not differ greatly from the development followed by Gent and Leach. We have nonetheless derived a few general features of global modes which have not been previously discussed.

Although only a simple model of local baroclinic instability is treated in the present work, the ideas are quite general and extend readily to realistic baroclinic–barotropic flows (provided as always that the requirement of gradual zonal variation is met). Indeed, the eigenmodes of local barotropic instability emerging in numerical simulations conducted by Merkine and Balgovind (1983) have a spatial structure that is strikingly similar to that of the baroclinic modes described below; it thus seems possible that their results could be explained by a similar analysis. The barotropic theory would certainly be relevant to the theory of monsoon depressions proposed by Lindzen *et al.* (1983). In fact, these authors recognized the importance of absolute instability in determining the stability characteristics of local winds, though the relation was not quantified or made precise. Nor are the concepts restricted to quasi-geostrophic systems; they could be applied equally well to, say, local Kelvin–Helmholz instability. Finally, one might be tempted to analyze the intriguing results of Simmons *et al.* (1983) in terms of the ideas presented herein. However, owing to lack of clear separation of scales between the basic state and the instability, such an analysis would be unlikely to prove fruitful.

2. Mathematical formulation of the stability problem

We begin with the nondimensional equations describing quasi-geostrophic flow of a two-layer fluid on the beta-plane. Let $L_d = (g\Delta\rho D/\rho_0 f_0^2)^{1/2}$ be the deformation radius based on layer depth D, and let U be an as yet unspecified velocity scale. If we nondimensionalize lengths by L_d, velocities by U and times by L_d/U, the equations of motion become

$$\partial_t q_j + J(\psi_j, q_j) = 0, \quad j = 1, 2, \tag{2.1}$$

where $j = 1$ corresponds to the upper layer, $j = 2$ corresponds to the lower layer, ψ_j is the streamfunction and q_j is the potential vorticity, which is given by

$$q_j = \nabla^2\psi_j - (-1)^j(\psi_2 - \psi_1) + \beta y. \tag{2.2}$$

In (2.2) $\beta = \beta_* L_d^2/U$ is the nondimensional beta-parameter, where β_* is the dimensional planetary vorticity gradient. Next, we linearize the equations of motion about a stationary state $\bar{\psi}_j(x, y)$ with corresponding potential vorticity

$$\bar{q}_j(x, y) = \nabla^2\bar{\psi}_j - (-1)^j(\bar{\psi}_2 - \bar{\psi}_1) + \beta y. \quad (2.3)$$

Upon substituting

$$\left.\begin{aligned} \psi_j &= \bar{\psi}_j(x, y) + \psi'_j(x, y, t) \\ q_j &= \bar{q}_j(x, y) + q'_j(x, y, t) \end{aligned}\right], \quad (2.4)$$

into (2.1) and neglecting terms quadratic in the perturbation quantities, the linearized equations of motion are found to be

$$\partial_t q'_j + J(\bar{\psi}_j, q'_j) + J(\psi'_j, \bar{q}_j) = 0, \quad (2.5)$$

where

$$q'_j = \nabla^2\psi'_j - (-1)^j(\psi'_2 - \psi'_1). \quad (2.6)$$

An arbitrarily chosen $\bar{\psi}_j$ generally will not be a stationary solution to (2.1). However, any state can be made stationary through the introduction of a suitable stationary vorticity source, as was done in Frederiksen (1983).

We now restrict attention to a special basic state which describes a zonal flow in each layer whose strength varies slowly in the zonal direction. To this end we introduce a slow zonal scale $X = \epsilon x$, where $\epsilon \ll 1$, and set

$$\bar{\psi}_j = -U_j(X)y, \quad (2.7)$$

in which y is to be regarded as an O(1) quantity. The zonal wind described by (2.7) has no horizontal shear, so that local barotropic instability is precluded. Nevertheless, (2.7) is sufficiently general as to allow localized regions of high baroclinicity, which is the configuration of primary interest. The general situation we wish to treat is depicted in Fig. 1.

Upon substituting (2.7) into (2.3), the basic-state potential vorticity becomes

$$\bar{q}_j = \Delta_j(X)y + O(\epsilon^2), \quad (2.8)$$

where

$$\Delta_j(X) = \beta + (-1)^j(U_2 - U_1), \quad (2.9)$$

whence the second Jacobian in (2.5) becomes

$$J(\psi'_j, \bar{q}_j) = (\partial_x\psi'_j)\Delta_j(X) - \epsilon(\partial_y\psi'_j)(\partial_X\Delta_j)y + O(\epsilon^2). \quad (2.10)$$

Likewise, the first Jacobian becomes

$$J(\bar{\psi}_j, q'_j) = -\epsilon(\partial_X U_j)(\partial_y q'_j)y + U_j\partial_x q'_j + O(\epsilon^2). \quad (2.11)$$

Combining these two results, the perturbation equation is

$$(\partial_t + U_j\partial_x)q'_j + (\partial_x\psi'_j)\Delta_j = \epsilon y[(\partial_y\psi'_j)(\partial_X\Delta_j) + (\partial_X U_j)(\partial_y q'_j)]. \quad (2.12)$$

In general, the $O(\epsilon)$ term in (2.12) must be retained if one wishes to follow the evolution of a wave packet as it propagates through the inhomogeneous medium. This is because the basic state varies appreciably only over zonal distances of $O(1/\epsilon)$; hence, a wave packet moving at O(1) speed requires a time of $O(1/\epsilon)$ to traverse the inhomogeneous region. Consequently, the approximate equations used must remain valid out to $t = O(1/\epsilon)$. This is also the time scale required for the initial perturbation to evolve into an eigenmode.

If the initial perturbation is y-independent, though, the $O(\epsilon)$ term in (2.12) vanishes identically, and the solution remains y-independent out to $t = O(1/\epsilon)$ because the coefficients of the lhs of (2.12) are independent of y. In this case, (2.12) takes the form

$$(\partial_t + U_j\partial_x)q'_j + (\partial_x\psi'_j)\Delta_j = 0, \quad (2.13a)$$

where

$$q'_j = \partial_{xx}\psi'_j - (-1)^j(\psi'_2 - \psi'_1), \quad (2.13b)$$

and the form of Δ_j given in (2.9) remains the same. The remainder of this paper will deal primarily with the properties of (2.13). Although the system is highly

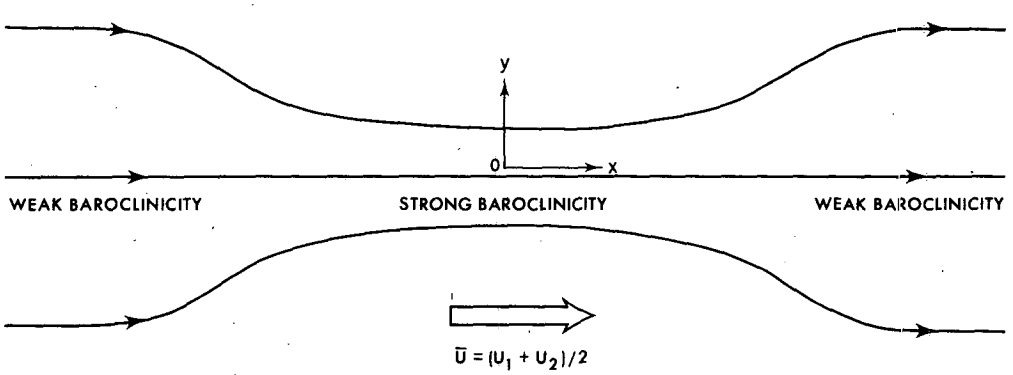

FIG. 1. Plan view illustrating the general character of the basic states examined in the stability study. The contours represent either upper level streamlines or contours of constant interface height (analogous to potential temperature in a continuously stratified model). The zonal wind is independent of y and the vertical mean of the zonal wind flows from left to right.

idealized, it retains all the features necessary for the investigation of the issues raised in the Introduction. It is important to note that (2.13) has precisely the same form as the conventional system describing instability of zonally homogeneous two-layer flow, save that the coefficients U_1, U_2, Δ_1 and Δ_2 are allowed to vary slowly in x.

The system (2.13) describes a one-dimensional marching problem which is readily integrated forward in time by numerical means. Of course, the integration must be carried out in a zonal domain finite in x, with appropriate boundary conditions at the endpoints of the domain. It is most convenient to impose cyclic boundary conditions, so that all quantities are assumed periodic with period L, where L is the width of the domain. This choice enables us to investigate global modes, in which the wave packet passes repeatedly through the baroclinic zone. In order to simulate the effects of a zonally infinite domain, we have provided for a sponge region occupying the first third of the computational domain. Within the sponge region, an artificial damping is introduced, with damping coefficient increasing from zero at the edges of the sponge region to a maximum value at its center. The sponge region absorbs virtually all energy leaving the right-hand boundary of the domain, thereby suppressing global modes. Most of the local modes we will consider, however, have infinitesimal amplitude at the computational boundaries and are therefore essentially unaffected by the cyclic boundary conditions. In such cases, we have found the inclusion of the sponge region to have virtually no effect on the modes.

With cyclic boundary conditions, the system is most easily solved using spectral transform techniques. All results to be presented below were computed using 512 Fourier modes in a domain extending from $x = -20\pi$ to $x = 20\pi$. In all cases, we show only the lower-level streamfunction perturbation $\psi'_2(x, t)$.

3. A review of the theory of absolute and convective instability

Because the concept of absolute instability figures so prominently in the subsequent discussion, it is necessary to digress for a review of the rudiments of the theory. We follow the development of Merkine and Shafranek (1980) quite closely, and the reader is referred to that work for a more complete review. Consider the evolution of one-dimensional linear waves in the domain $-\infty < x < \infty$. Suppose that the dispersion relation for the system is

$$\omega = \omega(k), \tag{3.1}$$

where ω is the frequency corresponding to wavenumber k. We allow ω to be complex, so that unstable waves can be treated. The evolution of a general wave packet is then given by

$$\psi(x, t) = \int_{-\infty}^{\infty} A(k) e^{i(kx - \omega(k)t)} dk, \tag{3.2}$$

where $A(k)$ is determined by initial conditions. It can be shown that the asymptotic form attained by the wave packet as $t \to \infty$ with x/t bounded is

$$\psi(x, t) \sim A(k_s)\sqrt{2\pi} e^{-i(\pi/4)} \frac{e^{i[(x/t)k_s - \omega(k_s)]t}}{(d^2\omega/dk^2|_{k_s})^{1/2} t^{1/2}}, \tag{3.3}$$

where $k_s(x/t)$ is determined by the equation

$$\left.\frac{d\omega}{dk}\right|_{k_s} = \frac{x}{t}. \tag{3.4}$$

Equations (3.3) and (3.4) represent a generalization of the well-known stationary phase approximation to the case of complex ω, corresponding to an unstable system. According to these formulae, $\mathrm{Im}[\omega(k_s) - (x/t)k_s]$ gives the growth rate following the ray x/t = const. Two rays are of particular interest. The first is the ray associated with the value of k where

$$\frac{d\omega_i}{dk} = 0. \tag{3.5}$$

Recalling that ω_i is the growth rate of the disturbance, we see that this k corresponds to the real wavenumber at which the maximum growth rate is attained; it is the "most unstable wavenumber" as conventionally defined and will therefore be designated k_m. Appealing to (3.4), the ray along which the maximum growth rate is attained is defined by

$$\frac{x}{t} = \left.\frac{d\omega_r}{dk}\right|_{k_m}. \tag{3.6}$$

Thus, the *peak* of the wave packet grows with the growth rate of the most unstable normal mode and moves with the speed of the group velocity evaluated at the most unstable wavenumber.

The second ray of special interest is that corresponding to the behavior at *fixed* x as $t \to \infty$, so $x/t \to 0$. From (3.4) the value of k_s for this ray is determined by solving the equation

$$\left.\frac{d\omega}{dk}\right|_{k_s} = 0. \tag{3.7}$$

Henceforth, we shall denote this special k_s by k_0. It is important to note that, since $\omega(k)$ is complex, k_0 must generally be complex as well. According to (3.4), the form of disturbance remaining in a fixed range of x after a sufficiently long time is

$$\psi(x, t) \sim A(k_0)\sqrt{2\pi} e^{-i(\pi/4)} \frac{e^{-i\omega(k_0)t} e^{ik_0 x}}{(td^2\omega/dk^2|_{k_0})^{1/2}}. \tag{3.8}$$

Thus, the disturbance at fixed x grows with growth rate $\omega_i(k_0)$, which may be called the "absolute" growth rate. The absolute growth rate can be zero or negative even when $\omega_i(k_m)$ is positive. When $\omega_i(k_0)$ is positive, the system is said to be *absolutely unstable.* If $\omega_i(k_0)$ is negative or zero while $\omega_i(k_m)$ is positive, the system is said to be *convectively unstable.* Another noteworthy feature of (3.8) is that, because k_0 is complex, the disturbance grows exponentially in space in some direction (presumably toward the peak of the wave packet). What we see here is essentially the structure of the tail of the wave packet that has been left behind after the peak has moved away.

It may be helpful at this point to show how these ideas manifest themselves in the evolution of some actual unstable wave packets. To this end, we discuss two simulations performed with the two-layer model described in Section 2. For these examples, the basic-state flow is taken to be *zonally uniform.* Units of velocity are chosen such that the shear $U_1 - U_2 = 1$. The sponge region was not included in these simulations, so that a wave packet leaving the right-hand boundary of the domain will reenter the domain from the left; calculations were terminated before this effect could contaminate the results. Both cases were carried out with $\beta = 0.25$. In the first case, we set $\bar{U} = (U_1 + U_2)/2 = 0.2$, which can be shown to result in absolute instability for the aforementioned β. In the second case, we set $\bar{U} = 1.5$, which can be shown to result in a convectively unstable system. In each case, the initial perturbation consisted of a Gaussian disturbance of the lower-level streamfunction field centered on $x = 0$. The wave packets shown are plotted with a logarithmically transformed ordinate, in order to make the structure of the tails visible.

In Fig. 2 we show the time evolution of the wave packet for the case $\bar{U} = 0.2$. The peak grows exponentially and moves downstream, but leaves behind in its wake a tail that also grows exponentially, albeit at a slower rate. The point to be emphasized is that the disturbance at $x = 0$, the site of the initial excitation, grows in time. This state of affairs may be contrasted with the case $\bar{U} = 1.5$, shown in Fig. 3. Here the peak grows at the same rate, but moves downstream more rapidly. In this case, though, the wake left at $x = 0$ does not grow with time.

These zonally homogeneous examples reveal a certain triviality of the notion of absolute instability from a physical standpoint. Regardless of whether the disturbance grows at fixed x, the peak grows with the usual normal-mode growth rate. In any zonally homogeneous physical situation, the rapidly growing peak will soon come to dominate the evolution of the flow. In a zonally inhomogeneous flow, however, the concept of absolute instability is more powerful. Here, what *would have been* the peak can move out of the unstable region into a region of lesser instability where its growth rate is reduced. If the reduction in growth rate is sufficient, the growth rate of the erstwhile tail can come to dominate the growth rate of the former peak, whereupon the "tail" becomes the site of maximum amplitude of the mode. It is in this situation that we expect a locally confined eigenmode to evolve. In a sense, then, it can be said that considerations of zonal inhomogeneity lend physical importance to the concept of absolute instability. This idea will be made more precise later in this paper.

4. Eigenmodes for zonally inhomogeneous flow: Numerical results

In this section, the system described in Section 2 is used to numerically compute the eigenmodes and eigenvalues of two families of zonally inhomogeneous flow. For each flow under consideration, we integrated the perturbed system forward in time until the most unstable eigenmode emerged. This technique restricts us to considering only the most unstable mode for each flow, but has the virtue of making it practical to use very high resolutions in the computation of the eigenmodes. After a sufficiently long time, the fastest growing mode (if there is a single such mode) dominates the evolution, and the perturbation field assumes the form

$$\psi_j' = [A_r^{(j)}(x)\cos\omega_r t - A_i^{(j)}(x)\sin\omega_r t]e^{\omega_i t}, \quad (4.1)$$

where $A_r(x)$ and $A_i(x)$ are the real and imaginary parts of the eigenmode. The growth rate ω_i was determined by computing a long-term average of the growth of the perturbation kinetic energy. Independently, A_r, A_i and ω_r were determined at each x by performing an exact fit to the local time evolution; the consistency of ω_r from one point to another was used as a check on the assumption that the time evolution had achieved the form of an eigenmode.

The velocity profiles were taken to be of the form

$$\left.\begin{aligned} U_1(x) &= \bar{U} + DU(x)/2 \\ U_2(x) &= \bar{U} - DU(x)/2 \end{aligned}\right\}, \quad (4.2)$$

where the mean flow $\bar{U}$ is independent of x. In each series of experiments we keep the vertical shear profile $DU(x)$ fixed and examine the stability properties of the flow as a function of mean flow $\bar{U}$. Of course, for zonally homogeneous flow this dependence is trivial. We will see that the effect of U in the zonally inhomogeneous case is far more interesting.

We consider profiles which are symmetric about the middle of the domain, so that $DU(-x) = DU(x)$. We assume further that the maximum shear, and hence the maximum baroclinicity, is attained at $x = 0$. All velocities are nondimensionalized by the maximum shear, so that $DU(0) = 1$. In these units, the Phillips criterion for conventional normal mode

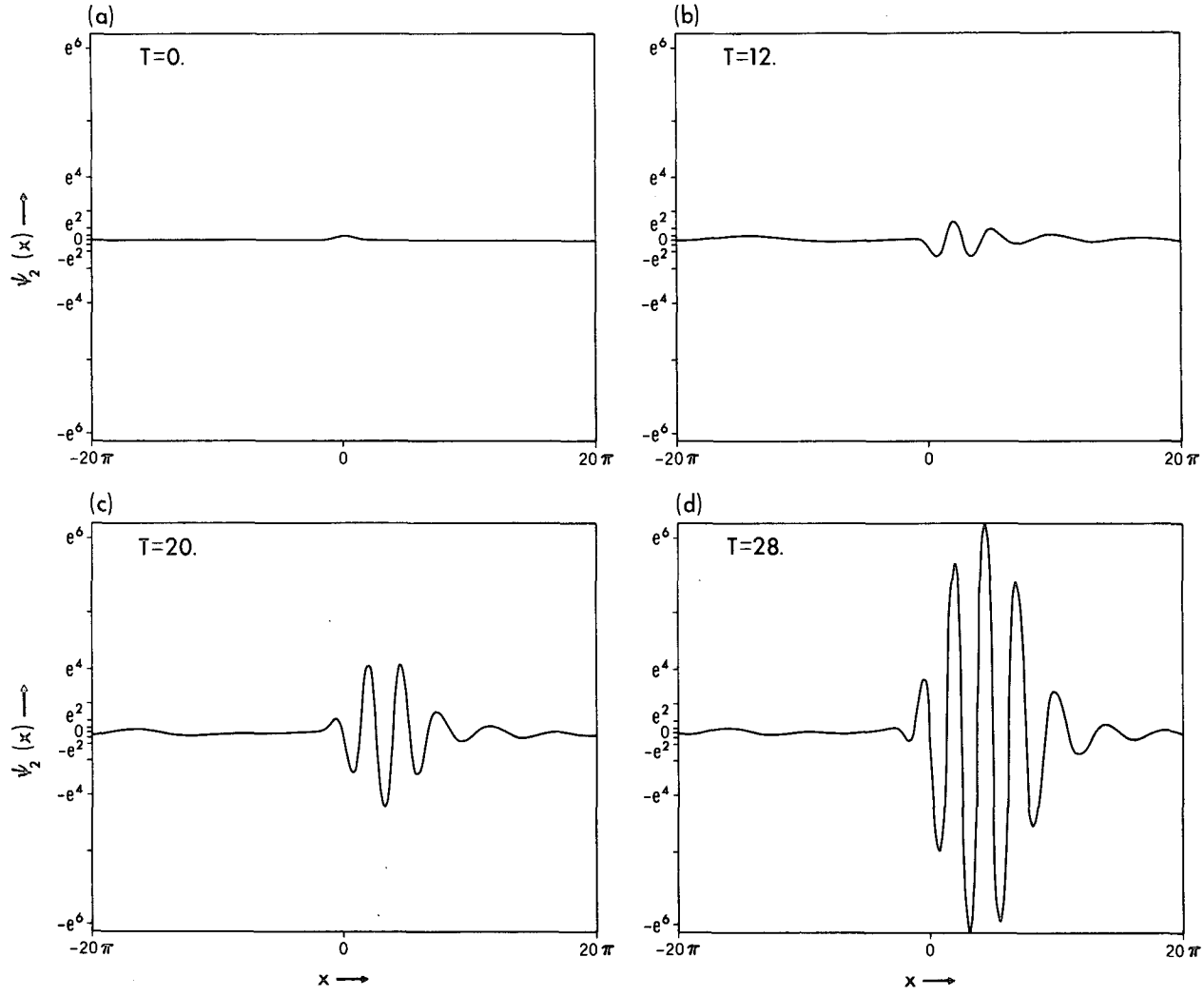

FIG. 2. Time sequence of wave packet evolution in zonally uniform flow in the absolutely unstable case $\bar{U} = 0.2$, $\beta = 0.25$. (a) $T = 0$, (b) $T = 12$, (c) $T = 20$, (d) $T = 28$. The horizontal axis is the zonal coordinate x and the vertical axis is the lower layer streamfunction. Note the logarithmically transformed ordinate.

instability of a *parallel* flow with nondimensional shear DU is simply

$$DU > \beta. \tag{4.3}$$

All the calculations to be discussed in this section were performed with $\beta = 0.25$. The maximum shear in the domain is then four times the critical shear; this is not atypical of actual shears observed locally in the atmosphere. In any event, we have found that other values of β yield qualitatively similar results.

The two profiles of $DU(x)$ studied are shown in Fig. 4. Both are chosen to be slowly varying with respect to the characteristic length scale of the unstable eddies, which is ~ 1 in the nondimensional units used here. For Profile 1 $DU(x) \to 0$ for large $|x|$; in this profile there is no energy source at large $|x|$ and the flow there can support only a spectrum of neutral Rossby waves. For Profile 2 $DU(x) \to 0.5$ at large $|x|$; this profile is unstable at large $|x|$ according to the local Phillips criterion. It will be seen that Profile 2 can nevertheless support localized baroclinic instability modes that decay to zero at large $|x|$.

We will deal with both local and global instabilities, though the emphasis will be on the former. Local instabilities are distinguished by the fact that they do not require periodic recycling of energy through the baroclinic zone for their existence. Therefore, it is a convenient idealization to think of them as existing in a zonally infinite domain, in which the streamfunctions satisfy the boundary condition

$$\psi_j' \to 0 \quad \text{as} \quad |x| \to \infty. \tag{4.4}$$

As stated in Section 2, the numerical computation was actually carried out subject to periodic boundary conditions. Therefore, in order to reproduce the

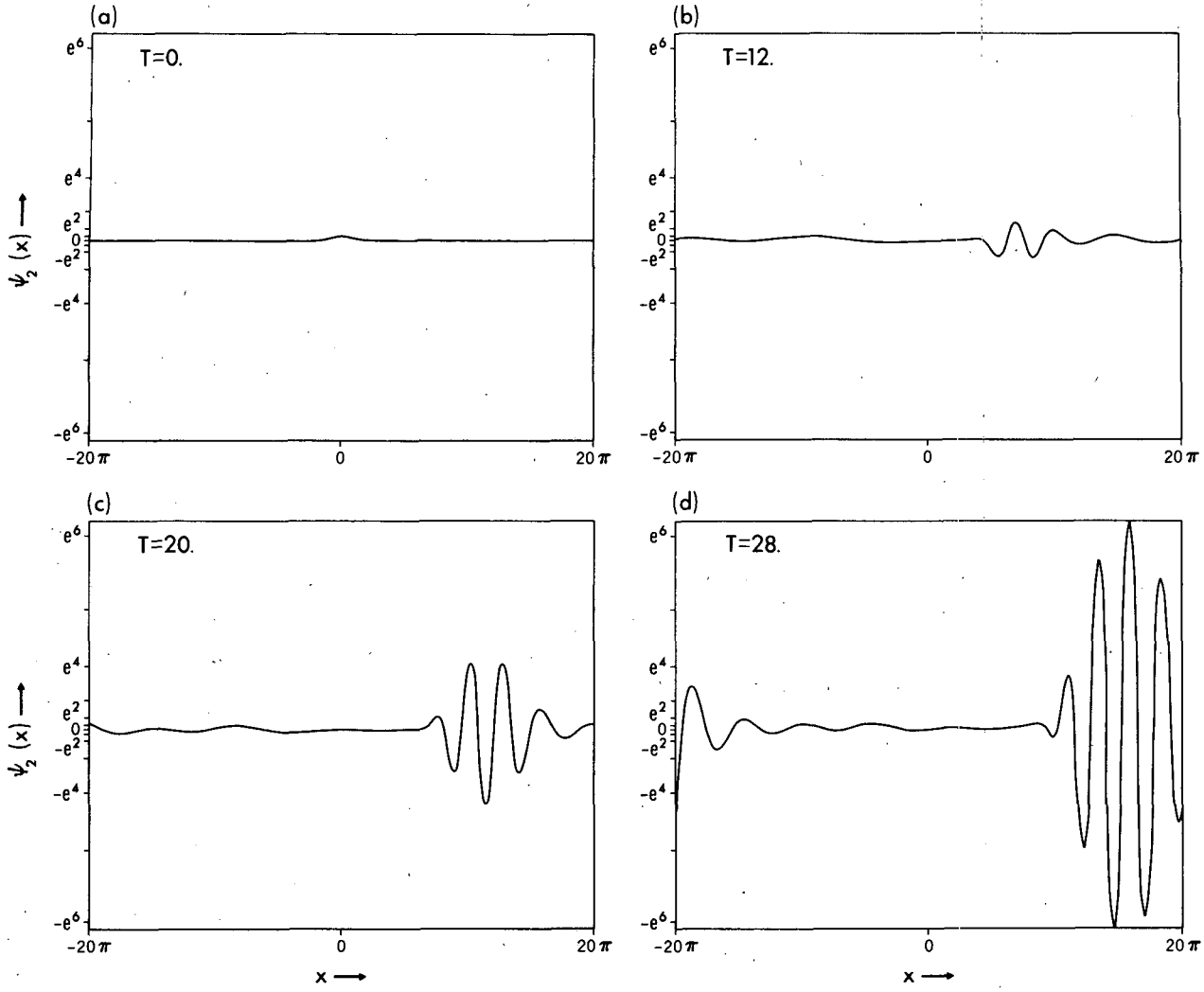

FIG. 3. As in Fig. 2; but for the convectively unstable case $\bar{U} = 1.5$.

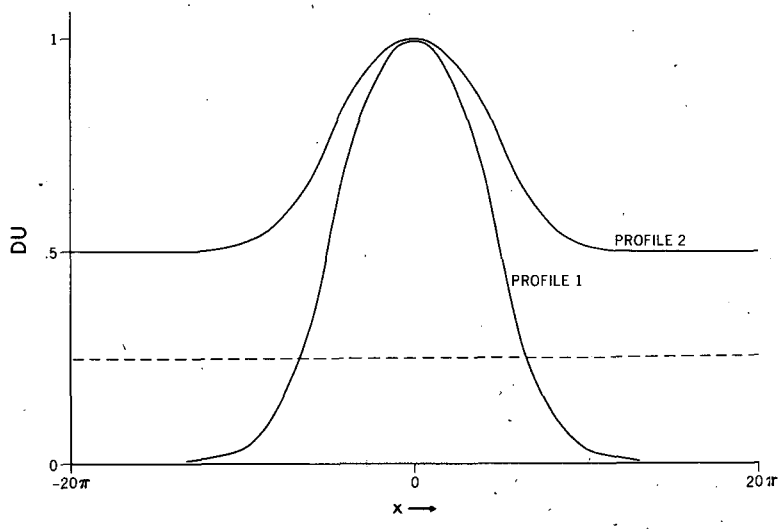

FIG. 4. The zonal structure of the two profiles of shear $DU(x)$ used in the numerical study.

effects of a zonally infinite domain, it is necessary to suppress the spurious recycling of energy leaving the right-hand boundary of the computational domain. This was achieved by introducing a sponge region between $x = -20\pi$ and $x = -6.666\pi$ designed to absorb essentially all energy entering the domain from the left. It is important to note that the sponge region is a computational device, and that a dissipating region is not really necessary for the existence of local modes in a periodic domain of sufficiently large period. In particular, if the mode is sufficiently localized that its amplitude decays to essentially zero before the computational boundaries are reached, then the periodic boundary conditions will have little effect on its structure or eigenvalue. The sponge region, then, serves two computational purposes. Firstly, it eliminates the global modes and allows the most unstable local mode to emerge in cases where a global mode would otherwise be dominant. Secondly, it eliminates "wraparound" of local modes that are too weakly localized to decay to zero at the right-hand boundary. Because of the large computational domain chosen, the latter situation was rarely encountered. Finally, in parameter ranges where global modes were dominant, they were computed by setting the sponge dissipation to zero, to allow the recycling of energy.

It is our intent in the following to make use of idealized flows, in order to develop some general principles concerning growth rate and modal structure which may then be applied to somewhat more realistic circumstances. The zonal scale within which modes are localized is of particular interest, as it determines the circumstances in which local modes can occur in the real atmosphere. Specifically, for the modes to be physically significant, the scale of localization must be less than the zonal separation between consecutive regions of high baroclinicity in the atmosphere. The localization scale can suggest, for example, when distinct Atlantic and Pacific storm tracks can exist. Similarly, the global mode computation serves to illustrate the general effects of global recycling of energy on growth rate and modal structure, although the period of the domain (dimensionally 40π radii of deformation) is considerably greater than any plausible zonal scale that can exist on the earth.

With these preliminaries behind us, we first turn to the numerical results for Profile 1, which has vanishing baroclinicity at infinity. The sponge region was included, and eigenmodes and eigenvalues were computed for several different values of the mean flow $\bar{U}$. In Fig. 5a we show the growth rates as a function of $\bar{U}$. The most important feature is that the growth rate is greatest at $\bar{U} = 0$ and falls off rather sharply as $\bar{U}$ is increased. This result stands in contrast to the situation obtaining in the more familiar case of baroclinic instability of zonally homogeneous flow, in which the growth rate is independent of the mean

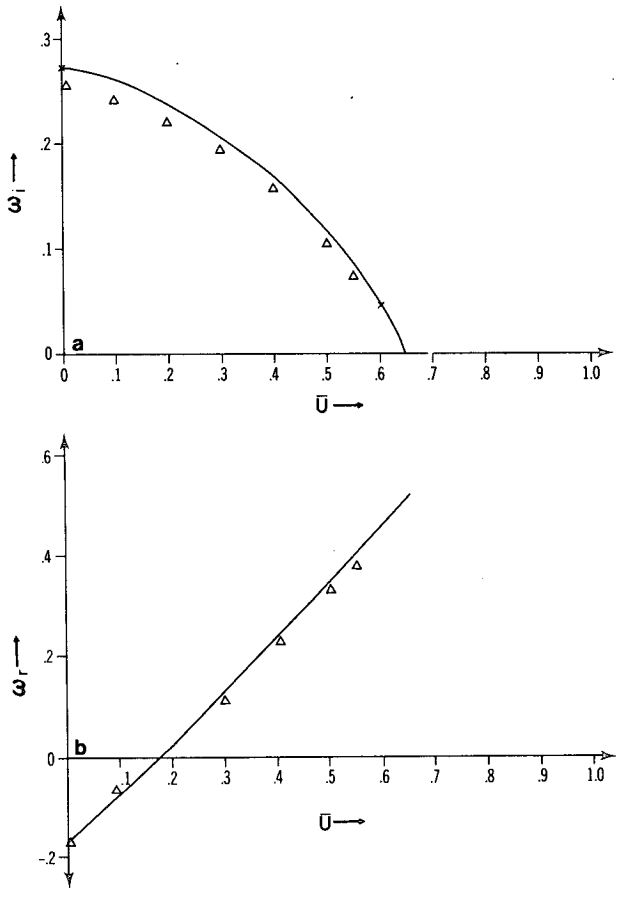

FIG. 5. Eigenvalues for Profile 1. The solid curves give the values associated with absolute instability at the point of maximum baroclinicity, while the triangles give the numerically computed results for the zonally inhomogeneous flow. (a) growth rate ω_i, (b) frequency ω_r.

flow. It also demonstrates that the local supercriticality with regard to the Phillips criterion is not a useful measure of the degree of instability of zonally inhomogeneous flow, as this quantity [$DU(0) - \beta$ in our units] is insensitive to the mean flow. The falloff of growth rate with $\bar{U}$ is, however, suggestive of the behavior of *absolute* growth rate, as defined in Section 3. In order to make the comparison quantitative, we calculated as a function of $\bar{U}$ the absolute growth rate of a *zonally homogeneous* flow with vertical shear $DU(0)$. The absolute growth rate was calculated by substituting the two-layer dispersion relation into (3.7) and solving for k_0, as was done by Merkine and Shafranek (1980). The shear at $x = 0$ was selected because for fixed $\bar{U}$, the maximum absolute growth rate occurs where DU (and hence baroclinicity) is greatest. The curve of absolute growth rate ω_{iabs} as a function of $\bar{U}$ is plotted along with the numerical results in Fig. 5a. It is seen that the numerical results for the zonally inhomogeneous flow follow the curve of maximum locally determined absolute growth rate

very closely. In Fig. 5b we show the frequency ω_r of the dominant eigenmode for Profile 1 as a function of $\bar{U}$, as revealed by the numerical computation. We also show the curve $\omega_{rabs}(\bar{U})$ which gives the frequency of the absolute mode associated with $DU(0)$. The agreement between the numerical results for zonally

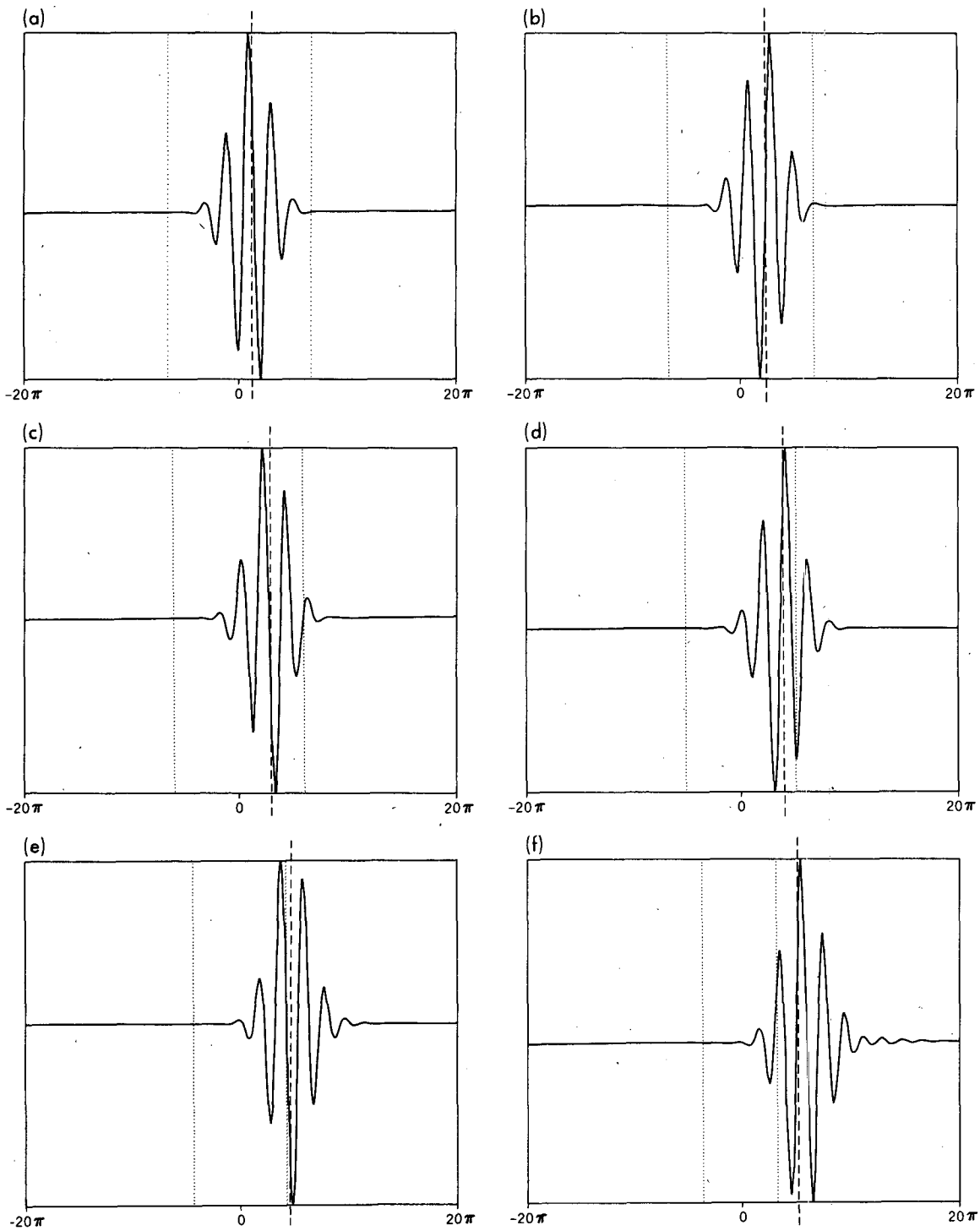

FIG. 6. Eigenmodes for Profile 1. The real part of the lower level perturbation streamfunction is shown. Values of $\bar{U}$ are: (a) 0.0, (b) 0.1, (c) 0.2, (d) 0.3, (e) 0.4 and (f) 0.5. Vertical dotted lines give outer boundaries of the absolutely unstable region. The vertical dashed lines give the theoretical position of the peak (see Section 5b).

inhomogeneous flow and the results of absolute instability theory applied locally at the point of maximum baroclinicity is almost perfect. These comparisons strongly suggest that the instability of the nonparallel flow is controlled by the occurrence of absolute instability at the site of maximum baroclinicity. It should be noted that the sponge region is not essential to the existence of the modes described above. When the calculations were repeated without a sponge region, the results were almost identical except when $\bar{U}$ was made greater than approximately 0.55, whereupon a formerly suppressed global mode began to dominate the evolution.

In Fig. 6a–f we show the dominant eigenmodes of Profile 1 for $\bar{U}$ ranging from 0 to 0.5. Only the real parts of the lower layer perturbation streamfunctions are shown; in each case, the imaginary part has a large-scale envelope similar to that visible in the real part and differs only in a phase shift of the short waves within the envelope. The vertical dotted lines in each graph give the outer boundary of the domain within which the flow is absolutely unstable according to the local dispersion relation. The first feature to note is that the modes are indeed local; each has a well-defined peak and decays both upstream and downstream of the peak. The upstream decay is not an artifact of the sponge region; calculations without a sponge region produced essentially indentical results. For positive $\bar{U}$, the peak occurs downstream of the point of maximum baroclinicity, as in Frederiksen (1978, 1980, 1983). We see also that the downstream distance at which the peak occurs is sensitive to $\bar{U}$, increasing when $\bar{U}$ is increased; this phenomenon was not explored in Frederiksen's work. It is noteworthy that the modes for larger $\bar{U}$ shown here bear a strong resemblance to the eigenmodes of local *barotropic* instability computed by Merkine and Balgovind (1983). This suggests that the nonparallel baroclinic and barotropic systems may share a common mathematical foundation. Finally, we point out that there is no obvious relation between the domain of localization of the eigenmodes and the domain within which the flow is locally absolutely unstable. In fact, for $\bar{U} = 0.5$, the peak amplitude occurs outside the absolutely unstable region. The actual local property determining the position of the peak will be discussed in Section 5.

The same series of calculations was repeated for Profile 2, which is baroclinically unstable at large $|x|$. The growth rate as a function of $\bar{U}$ is shown in Fig. 7a and the frequency is shown in Fig. 7b. For reasons that will become clear shortly, results for $\bar{U} > 0.5$ are not shown. Note that the local absolute instability curves are identical to those in Fig. 5, as $DU(0)$ is unchanged. Using these curves as a reference point, it is evident that the numerically determined growth rates and frequencies are much the same for Profile 2 as for Profile 1, and likewise follow the locally

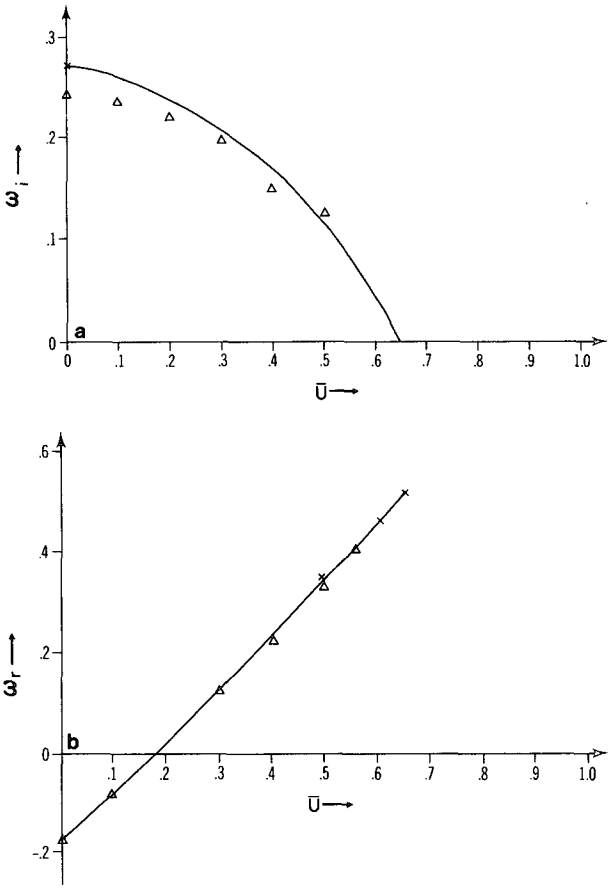

FIG. 7. As in Fig. 5, but for Profile 2.

determined absolute instability curves. This shows that the eigenvalues for these modes are determined locally by the flow properties near the point of maximum baroclinicity, and are relatively insensitive to the baroclinicity away from this point. This feature is very important, as it implies that *the growth rate of a local mode is determined by the maximum baroclinicity in the domain, and not by the average baroclinicity.*

The eigenmodes for Profile 2 are shown in Fig. 8a–f, in the same format as for Profile 1. Note that for $\bar{U} \leq 0.3$ the flow is not only unstable in the normal mode sense throughout the domain, but is actually *absolutely* unstable throughout the domain; nevertheless, localized modes exist. Hence, *vanishing absolute growth rate at infinity is not necessary for localization.* It is only necessary for the absolute growth at $x = 0$ to, in some sense, dominate the rate at which perturbations grow at infinity. The peaks shift downstream with increasing $\bar{U}$, as for Profile 1. In the Profile 2 cases, however, it can be clearly seen that as $\bar{U}$ increases and growth rate decreases, the spatial decay scale downstream of the peak becomes progressively greater. This phenomenon occurs in

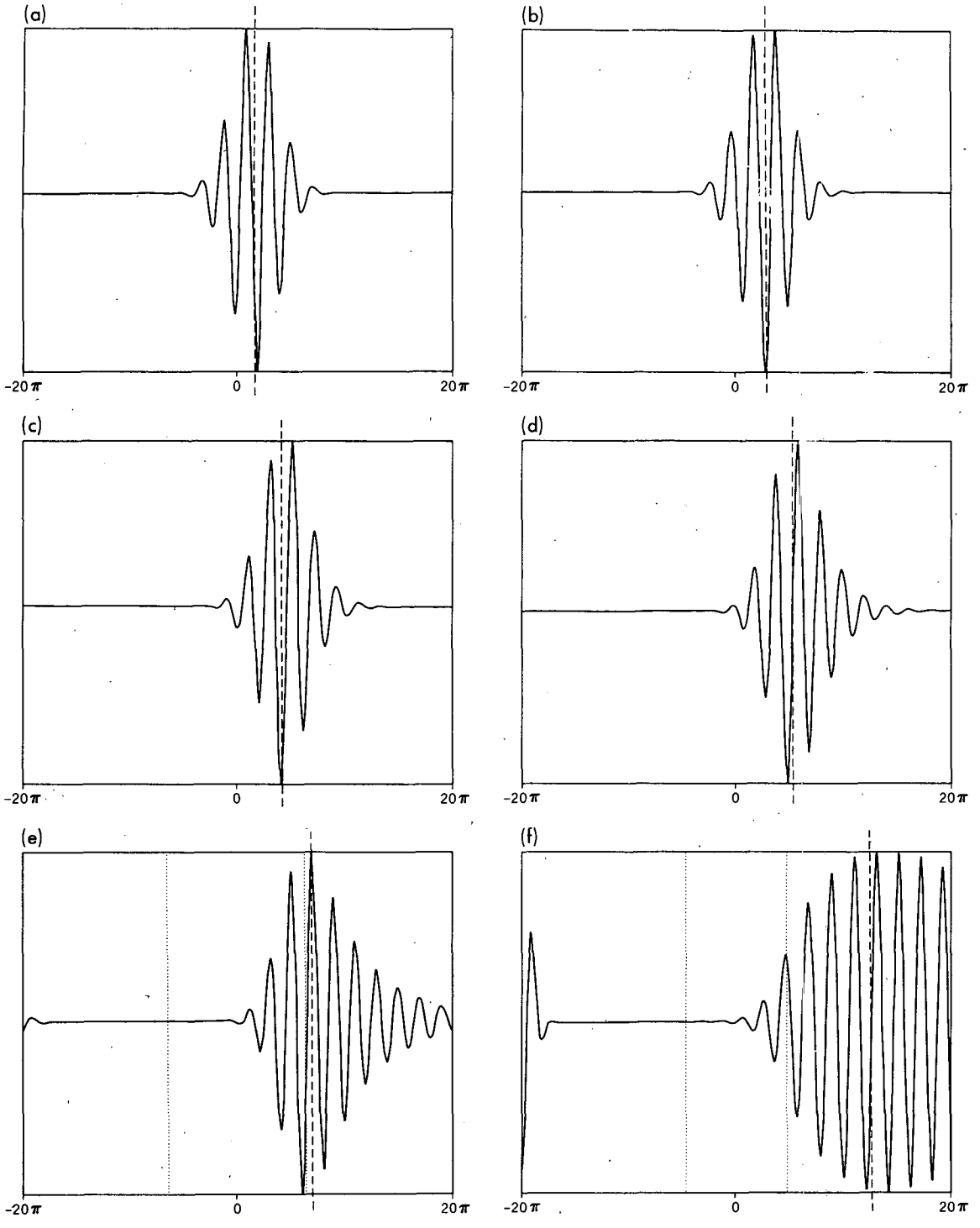

FIG. 8. As in Fig. 6, but for Profiile 2.

Profile 1 as well, but is not as evident in that case because the mode always decays so rapidly downstream of the peak that differences are difficult to detect by eye. The tendency for more weakly growing modes to extend further downstream was noted also in the barotropic case by Merkine and Balgovind (1983); they were able to explain the phenomenon simply in terms of the Rossby wave dispersion relation for the case in which the flow is unsheared at infinity. We see here that the same feature occurs even when

the flow has an energy source at infinity. A general discussion of the local properties determining the downstream decay scale will be given in Section 5. For $\bar{U} = 0.4$, the downstream decay scale becomes great enough that the sponge region plays a small role in preventing energy from reentering the domain from the left. At $\bar{U} = 0.5$, the downstream decay scale becomes essentially infinite; this mode is the "marginally localized mode" for Profile 2. Modes with larger $\bar{U}$ grow exponentially downstream until the sponge region is reached; such modes are artificially localized by the sponge region, and could not exist as local modes in a truly infinite domain. In an infinite domain, one would see the peak of the wave packet leaving the highly baroclinic zone grow more rapidly than the absolutely growing tail left behind; eventually, the propagating peak would come to dominate the evolution of the flow. This situation cannot occur for Profile 1, since wave packets leaving the baroclinic region in that case lose their energy source and stop growing. In general, upon comparing the results for Profile 1 and Profile 2, we find that the modes for Profile 2 decay more gradually downstream of the peak. Thus, *the contrast between maximum and minimum baroclinicity, in the flow determines the extent of localization of the eigenmodes, with high contrast favoring localization.*

The control of the growth rates of local modes by local absolute growth rate at $x = 0$ may seem odd in light of the fact that the peak amplitude of the eigenmodes occurs well downstream of $x = 0$. Our interpretation of this state of affairs is as follows. The absolute instability at $x = 0$ may be regarded as a "wavemaker" which introduces a sequence of wave packets, each of which has greater amplitude than the last. The peak of each wave packet grows in amplitude as it moves downstream, much as can be seen in the uniform flow case shown in Fig. 2. In the zonally inhomogeneous case, though, the growth rate of the peak decreases as it moves downstream. Past the point x_1 where the peak growth rate falls below the growth rate of successive disturbances released by the wavemaker (to be thought of as the local absolute growth rate at $x = 0$), the amplitude of the peak arising from the packet released at time t_n becomes less than the amplitude at x_1 of a packet released at an earlier time t_{n-1}. In this manner, the eigenmode attains a form that grows exponentially in space up to x_1 and thereafter decays. Admittedly, this argument is lacking in rigor. It does, however, predict the qualitative dependence of the peak position on $\bar{U}$. When $\bar{U} = 0$, the absolute growth rate is about the same as the normal-mode (peak) growth rate; hence, the normal-mode growth rate at $x = 0$ coincides with the absolute growth rate at $x = 0$, and the peak occurs there. When $\bar{U}$ is increased, the absolute growth rate at $x = 0$ decreases, but the local normal-mode growth rate at each x does not; hence, one must go to smaller values of DU (larger x) before the local normal-mode growth rate drops below the absolute growth rate found at $x = 0$. Accordingly, the peak shifts downstream. In this fashion, the absolute instability occurring at $x = 0$ may be regarded as the "seed" for instabilities which grow subsequently downstream. A more rigorous link between absolute instability, growth rate and position of peak amplitude will be presented in Section 5.

What happens when $\bar{U}$ is made so large that the flow becomes absolutely stable at the site of maximum baroclinicity? The answer depends on whether a sponge region is included. We have found numerically that when the sponge is included, the initial perturbation grows for a time, while it is still in the baroclinic zone, but eventually moves out into the sponge region leaving nothing behind. The wave packet then decays to zero, leaving an undisturbed basic state. Thus, with a sponge included the system becomes *stable* when the flow at the site of maximum baroclinicity becomes *absolutely stable.* This situation is nonphysical, unless one posits the existence of a strongly dissipative region in the real atmosphere. In an infinite zonal domain, in which no sponge would be necessary, the packet would move away to $x = \infty$ and the perturbation in any *fixed range* of x would eventually decay to zero; it is this sort of behavior that the sponge region is reproducing. What would happen in the real atmosphere depends on the postulated fate of the wave packet after it leaves the highly baroclinic zone. If it moves into a region of sufficiently weak baroclinicity, natural frictional effects may indeed be strong enough to cause it to decay, whence the results would be similar to our results including the sponge region. Otherwise, the wave packet continues to grow as it moves away from the highly baroclinic zone. In the real atmosphere, such a situation is likely to be governed by nonlinear processes of equilibration and decay. In a linearized model such as used in Frederiksen (1983), the wave packet can survive a circuit of the globe and reenter the original baroclinic zone, whereupon it commences a new period of rapid growth. Under these circumstances, we expect a global eigenmode to eventually evolve. We may say that the global modes are "self-seeded," whereas the local modes are seeded by *in situ* absolute instability.

In order to illustrate the nature of the global mode, we will discuss the results of an integration for the Profile 2 case with $\bar{U} = 1$ and the sponge dissipation set to zero. In Fig. 9 we show the state the streamfunction has attained at nondimensional time $T = 320$. This time is sufficient to allow a wave packet to complete roughly three circuits of the domain. Even at such a long time after the initial localized perturbation, the streamfunction has not yet attained the form of an eigenmode; while the frequency and growth rate have reached fairly steady values of 0.73

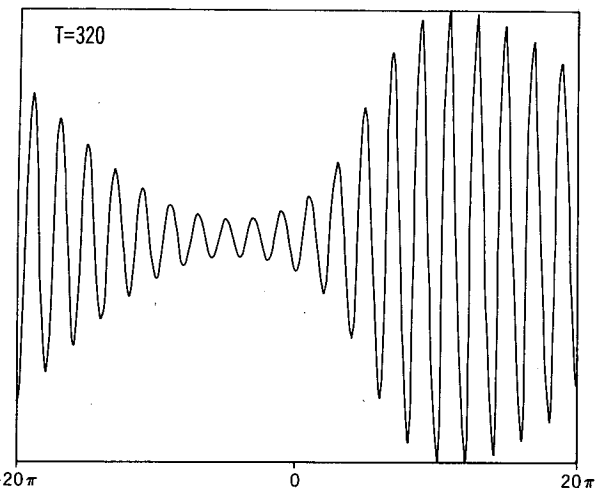

FIG. 9. Lower layer streamfunction at time $T = 320$ after initial perturbation of Profile 2 for convectively unstable case $\bar{U} = 1$. The sponge region is not included in this calculation. The perturbation at this time has not yet attained the form of an eigenmode.

and 0.16, respectively, the relative amplitude of the peak and the tail continue to undergo a slow oscillation (not shown). Indeed, the time scale of the oscillation is comparable to the time required for a packet to complete a circuit of the domain, and the overall pattern retains something of the character of a wave packet passing repeatedly through the baroclinic zone. Similar results were obtained for Profile 1 and for other absolutely stable values of $\bar{U}$. Nevertheless, the pattern in Fig. 9 clearly reveals the role of recycling of energy in maintaining the global mode; the tail of the mode extends far downstream of the peak and reenters the domain from the left, whereafter it enters the baroclinic zone and commences growing spatially toward the peak. The peak occurs downstream of the baroclinic zone, as it does for the local modes.

The difficulty in isolating an eigenmode by time-integration suggests that the system has two or more eigenmodes with very similar growth rates. Because of this difficulty, we defer further discussion of the global modes to Section 5, where we will see that this is, indeed, the case. The fact that a global eigenmode does not clearly emerge even after sufficient time for three circuits of the domain clearly indicates that the spatial structure of an individual global mode is of dubious relevance to the behavior of the real atmosphere. Reduced to the more familiar case of a zonally uniform basic state, this amounts to the statement that we would never expect baroclinic instability in the atmosphere to take the form of a single sinusoidal wave extending around the globe. In either case, the set of global modes is still useful in superposition for the representation of the transient evolution of a wave packet. In interpreting the results of zonally inhomogeneous stability calculations on the sphere, one must be wary of the possibility that some of the modes with sizable growth rates may be global modes which are likely to have different physical consequences than local modes.

5. Eigenmodes for zonally inhomogeneous flow: WKB analysis

a. Derivation of WKB equations

We wish to find the eigenvalues of (2.13) subject to suitable boundary conditions to be specified later. Substituting

$$\psi_j' = \hat{\psi}_j(x)e^{-i\omega t}, \quad j = 1, 2, \tag{5.1}$$

into (2.13), we obtain the eigenvalue problem

$$(-i\omega + U_j\partial_x)\hat{q}_j + (\partial_x\hat{\psi}_j)\Delta_j = 0, \tag{5.2a}$$

$$\hat{q}_j = \partial_{xx}\hat{\psi}_j - (-1)^j(\hat{\psi}_2 - \hat{\psi}_1), \tag{5.2b}$$

where U_j and Δ_j vary slowly in x, as before. We now make use of the slow variation of these coefficients to find an approximate solution to (5.2) which, together with boundary conditions, will determine the eigenvalue ω.

As in Section 2, we introduce the slow variable $X = \epsilon x$ and write $U_j = U_j(X)$ and $\Delta_j = \Delta_j(X)$. Next, we seek a solution of the form

$$\hat{\psi}_j = A_j(X)e^{iS(X)/\epsilon}, \tag{5.3}$$

where S is allowed to be complex. The factor $1/\epsilon$ in the exponential allows the phase and amplitude to vary by order unity amounts over order unity distances while keeping the *rate* of variation $\epsilon^{-1}dS/dx = dS/dX$ a function of the slow variable alone. This is the fundamental tenet of the WKB approximation, and must be checked *a posteriori*.

Equation (5.2) involves first, second and third derivatives of the streamfunctions. For modes of the form (5.3), these derivatives become

$$\partial_x\hat{\psi}_j = (iS'A_j + \epsilon A_j')e^{iS/\epsilon}, \tag{5.4a}$$

$$\partial_{xx}\hat{\psi}_j = [-S'^2A_j + i\epsilon(S''A_j + 2S'A_j')]e^{iS/\epsilon} + O(\epsilon^2), \tag{5.4b}$$

$$\partial_{xxx}\hat{\psi}_j = [-iS'^3A_j - 3\epsilon S'(S''A_j + S'A_j')]e^{iS/\epsilon} + O(\epsilon^2), \tag{5.4c}$$

where $S' = dS/dX$, $S'' = d^2S/dX^2$ etc. It is presumed that S', S'' and A' are order unity quantities. Upon substituting (5.3) into (5.2) and making use of (5.4), the lowest order approximation to the system becomes

$$\left(-\frac{\omega}{S'} + U_j\right)(-S'^2A_j - (-1)^j(A_2 - A_1)) + A_j\cdot\Delta_j = 0; \quad j = 1, 2. \tag{5.5}$$

Note that at each X this equation is identical in form to the conventional two-layer stability equations

[Pedlosky, 1979, Eq. (7.11.4)] except that S' appears where we would ordinarily have the wavenumber k. The approximation was constructed to assure that this would be the case. To emphasize the similarity, we define the local wavenumber

$$k = S'(X), \tag{5.6}$$

and henceforth refer to k in place of S'. S is obtained by integration; in terms of the untransformed variable x, (5.3) attains the familiar WKB form

$$\hat{\psi}_j = A_j(X)e^{i\int_{x_0}^{x} k\,dx}, \tag{5.7}$$

where x_0 is a constant of integration. The next order correction to S would alter only the slowly varying amplitude factor multiplying the exponential. All that remains is to determine $k(X)$.

We may apply the conventional two-layer dispersion relation [(Pedlosky, 1979, Eq. (7.11.13)] at each X to relate k and ω. Thus,

$$\frac{\omega}{k} = \bar{U} - \frac{\beta(k^2+1)}{k^2(k^2+2)} \pm \frac{[4\beta^2 - k^4 DU^2\cdot(4-k^4)]^{1/2}}{2k^2\cdot(k^2+2)}. \tag{5.8}$$

Recall that $\bar{U}$ and DU vary with X. This equation is not in a very suitable form for our purposes, as we wish to specify a constant (X-independent) ω and find $k(X)$. To this end, we write (5.8) as a polynomial in k with X-dependent coefficients:

$$\left[\bar{U}^2 - \tfrac{1}{4}DU^2\right]k^7 - [2\bar{U}\omega]k^6 + [\omega^2 + 4\bar{U}^2 - 2\beta\bar{U}]k^5 - [8\bar{U}\omega + 2\beta\omega]k^4 + [4\omega^2 + 4\bar{U}^2 - 6\beta\bar{U} + \beta^2 + DU^2]k^3 + [-8\bar{U}\omega + 6\beta\omega]k^2 + [4\omega^2 - 4\beta\bar{U} + 2\beta^2]k + [4\beta\omega] = 0. \tag{5.9}$$

Except when $\bar{U} = \pm DU/2$, this is a seventh-order equation, and therefore has seven complex roots k. Hence, within each region in which WKB is valid, (5.7) should be replaced by a sum of seven independent solutions, corresponding to the seven branches of k. We will see in Sections 5b and c that only a very few of these branches are physically meaningful. For any ω we can now find a WKB solution; the eigenvalue problem is completed by imposing boundary conditions on this solution.

Even if the coefficients DU and $\bar{U}$ are slowly varying, there are two ways the WKB approximation can break down. Firstly, if $k = S' \to 0$ at some X, then the leading term in, say, (5.4b) becomes comparable to the $O(\epsilon)$ term. This is the sort of breakdown encountered at a "classical turning point" in the familiar quantum mechanical applications of WKB theory. This cannot happen for unstable modes in the current problem though, since $S' = 0$ in (5.8) implies $\omega = 0$. Alternately, the ordering can break down if $S'' = dk/dX$ becomes infinite at some point while $S' = k$ remains finite; this can occur in the present problem.

b. Anatomy of the local modes

In order to study the local modes, we consider a zonally infinite domain $x \in [-\infty, \infty]$ and impose the boundary conditions

$$\hat{\psi}_j(x) \to 0 \quad \text{as} \quad |x| \to \infty. \tag{5.10}$$

We will consider profiles such that DU and $\bar{U}$ are asymptotic to constant values DU_∞ and $\bar{U}_\infty$ as $|x| \to \infty$. Since k depends on X through DU and $\bar{U}$ alone, this implies that *for any given branch* of k, $k(+\infty) = k(-\infty)$. Consequently, if the solution does not switch branches somewhere in the domain, the boundary condition (5.10) cannot be satisfied: If we make $k_i(+\infty) > 0$ so as to assure decay at positive x, then the mode will grow toward negative x, and, conversely, if we make $k_i(-\infty) < 0$.

When can the WKB solution switch branches? Under circumstances where WKB remains valid near the switching point, branch switching can occur only near a point X_c where the two branches merge. More precisely, we require the existence of a point X_c such that

$$k^{(1)}(X) \to k^{(2)}(X) \quad \text{as} \quad X \to X_c. \tag{5.11}$$

If this condition were not met, the derivatives of $\hat{\psi}_j$ would be discontinuous at the switching point even at leading order [see (5.4)]. Alternately, switching can occur at a point where $dk/dX \to \infty$ and WKB breaks down. We will see shortly that coalescence must generally occur in this case as well.

The situation near the coalescence point can be investigated for a *general* dispersion relation

$$F(k, \lambda) = 0 \tag{5.12}$$

of which (5.9) is a special case. Here λ represents any parameter of the problem; with regard to (5.9) it could be $\bar{U}$, DU or ω. All we require of F is that it be a differentiable function of its arguments, a requirement which is met by (5.9).

Now suppose there are two roots $k^{(1)}(\lambda)$ and $k^{(2)}(\lambda)$ that approach a common limit k_c as $\lambda \to \lambda_c$. Then,

$$\partial_k F(k, \lambda_c)|_{k_c} = \lim_{\lambda\to\lambda_c}\left\{\frac{F(k^{(1)}, \lambda) - F(k^{(2)}, \lambda)}{k^{(1)} - k^{(2)}}\right\} = 0, \tag{5.13}$$

where the numerator on the rhs vanishes identically because $k^{(1)}$ and $k^{(2)}$ are roots of (5.12). Consequently, (5.12) has the form

$$\tfrac{1}{2}[\partial_{kk}F(k_c, \lambda_c)](k - k_c)^2 + [\partial_\lambda F(k_c, \lambda_c)](\lambda - \lambda_c) = 0 \tag{5.14}$$

near λ_c, whence the roots have the local behavior

$$k = k_c \pm [2\partial_\lambda F(k_c, \lambda_c)/\partial_{kk} F(k_c, \lambda_c)]^{1/2}(\lambda - \lambda_c)^{1/2}, \tag{5.15}$$

provided that $\partial^2 F/\partial k^2$ does not vanish. Hence, viewed as a function of *any* parameter, the roots generally have a square-root branch point near the coalescence point.

For the problem at hand, this result has two important consequences. Suppose the dispersion relation has a coalescence point for some $(\bar{U}_c, DU_c) \equiv [\bar{U}(X_c), DU(X_c)]$ occurring in the domain. Then, from (5.15) k also has a square-root branch point when viewed as a function of ω. This implies that

$$\left.\frac{\partial \omega}{\partial k}\right|_{k_c} = 0. \tag{5.16}$$

With reference to (3.7), we see that the wavenumber at coalescence k_c is also the complex wavenumber of absolute instability corresponding to the local wind $(\bar{U}_c, DU_c)$ at the coalescence point, and $\omega_r(k_c)$ and $\omega_i(k_c)$ are the associated frequency and growth rate. Thus, for unstable modes *the condition for the existence of branch switching is identical to the condition for the existence of absolute instability at some point in the flow, as determined by the local winds, and the eigenvalue is determined by the characteristics of the absolute instability at that point.* The existence of branch switching is only a necessary condition for local instability; it remains to be seen whether local modes can be built up, even when the branch switching is allowed.

The second noteworthy result is that a coalescence point will, in general, be a WKB breakdown point. This is because $dk/dX = (dk/d\lambda)(d\lambda/dX)$ and $dk/d\lambda$ become infinite at the coalescence point according to (5.15). In this case, a different local analysis must be used to continue the solutions across the coalescence point; we have not attempted to solve the general connection problem for the two-layer model. In the special case in which $d\lambda/dX = 0$ at the coalescence point for all X-varying parameters in the problem, the difficulty is avoided and WKB remains valid through the coalescence point.

In the two-layer problem, WKB remains valid through the coalescence point if dDU/dX and $d\bar{U}/dX$ vanish there. The first condition is satisfied at the point of maximum baroclinicity. The second condition is trivially satisfied for the profiles studied in Section 4, where $\bar{U}$ is constant. More generally, for physically plausible profiles, $\bar{U}$ will have a maximum at the same place as DU, since surface friction holds the low-level winds near zero, making U a roughly monotonic function of DU. Except when U falls off very sharply from its maximum, the maximum absolute growth rate occurs at the point of maximum baroclinicity; this point is, therefore, the candidate coalescence point that determines the growth rate of the fastest growing mode.

We are now equipped to construct WKB approximations to the fastest growing local modes. Assuming that DU and $\bar{U}$ are maximized at $x = 0$, we seek a solution of the form

$$\hat{\psi}_j = \begin{cases} A_j e^{i\int_0^x k^+ dx} & \text{for } x \geq 0 \\ A_j e^{i\int_0^x k^- dx} & \text{for } x \leq 0, \end{cases} \tag{5.17}$$

where $k^+[DU(X), \bar{U}(X), \omega]$ and $k^-[DU(X), \bar{U}(X), \omega]$ represent two branches of the solution to (5.9) with the properties

$$\mathrm{Im}\{k^+[DU(\infty), \bar{U}(\infty), \omega]\} > 0, \tag{5.18a}$$

$$\mathrm{Im}\{k^-[DU(-\infty), \bar{U}(-\infty), \omega]\} < 0. \tag{5.18b}$$

The eigenvalue ω must be chosen to correspond to the absolute instability associated with $[U(0), DU(0)]$ so that the two branches coalesce at $x = 0$. Whether or not the two modes satisfy (5.18) must be checked by solving (5.9). The results are best explained in terms of an example. Figure 10 shows how the two

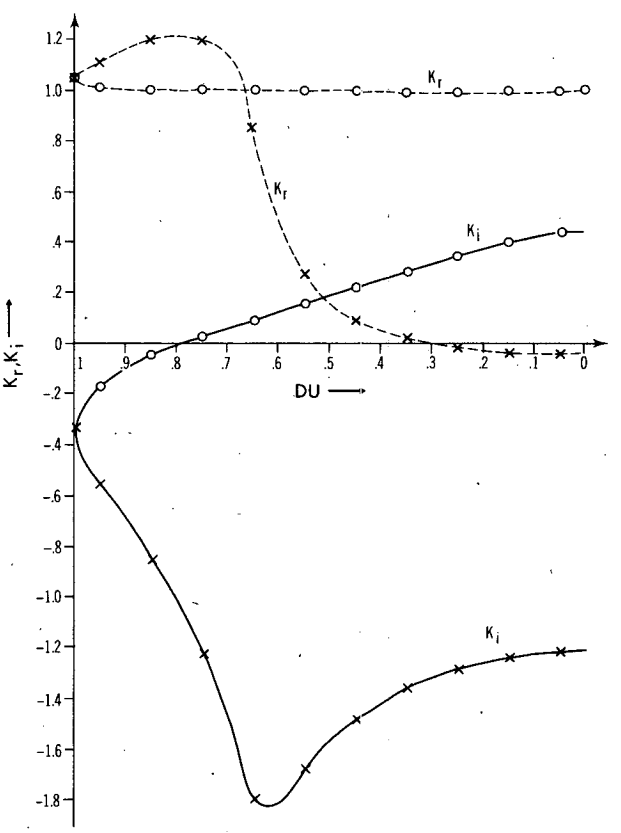

FIG. 10. Dependence of a complex wavenumber on vertical shear DU for two branches of the dispersion relation. In this calculation, $\beta = 0.25$, $\bar{U} = 0.3$ and ω is set equal to the value associated with absolute instability at $DU = 1$. The two modes are denoted k^+ and k^-. Dashed line with circles, k_r^+; solid line with circles, k_i^+; dashed line with crosses, k_r^-; solid line with crosses, k_i^-.

roots vary as DU is varied between unity and zero, in the case $U = 0.3$ and $\beta = 0.25$. Here ω is chosen so that coalescence occurs at $DU = 1$. For one root (call it k^+), the imaginary part k_i^+ is negative near $DU = 1$, but becomes positive for $DU < 0.8$; thus (5.18a) is satisfied provided $DU(\infty) < 0.8$. The mode grows downstream of $x = 0$ until the value of x is reached where DU falls below 0.8. The peak amplitude occurs there, and the mode decays to zero with larger x. The spatial decay rate becomes greater as $DU(\infty)$ is made smaller, in accordance with the numerical results of Section 4. This example illustrates the point that $DU(\infty)$ must fall below a certain critical value (0.8 in this case) in order for local modes to exist. Note also that the point where k_i^+ crosses zero is an ordinary WKB point, because k_r^+ remains finite there. The branch switching occurs at $x = 0$ and not at the peak. Finally, Fig. 10 shows that k_i^- is negative for all DU. In fact, it becomes very negative as DU is decreased from unity, indicating that the upstream decay is rapid. Apart from consistency with the assumption that $DU(0)$ be the maximum baroclinicity, localization imposes no constraint on the upstream baroclinicity $DU(-\infty)$.

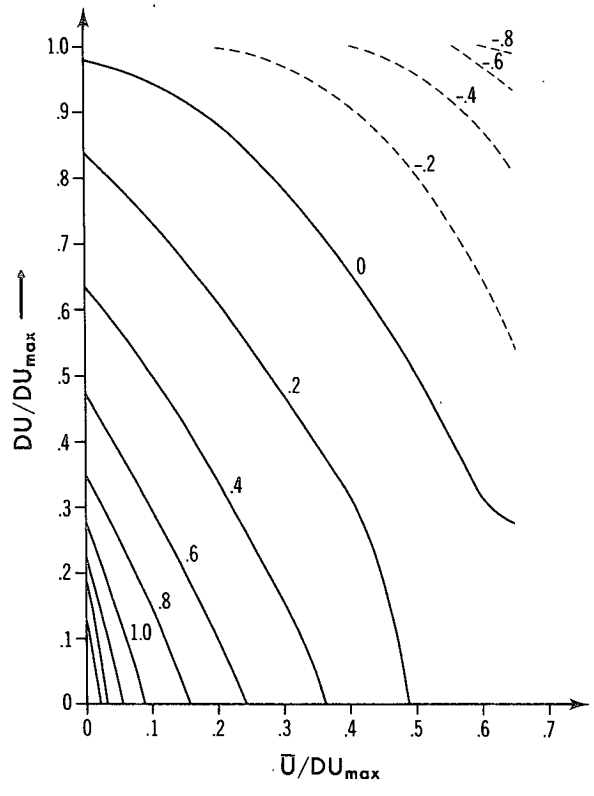

FIG. 11. Contours of constant k^+ in the (U, DU) plane for $\beta = 0.25$. DU_{max} refers to the maximum baroclinicity occurring in the domain and ω is set equal to the value associated with absolute instability at DU_{max}. Dashed contours indicate negative k_i^+, which corresponds to exponential downstream growth.

We have found the situation to be qualitatively similar in every respect for other values of β and $\bar{U}$ for which $DU(0)$ is absolutely unstable. In short, WKB theory predicts that *local modes having growth rate and frequency determined by absolute instability at the point of maximum baroclinicity exist whenever the downstream baroclinicity falls below a certain critical value that is a function of* $\bar{U}$ *and* β. The term $k_i^+(DU, \bar{U}, \omega)$ carries most of the interesting quantitative information about the structure of the modes. In Fig. 11 we show contours of k_i^+ in the $(DU, \bar{U})$ plane for $\beta = 0.25$. For each DU and $\bar{U}$, of course, we set $\omega = \omega_{abs}(DU_{max}, \bar{U})$ which is the theoretically determined eigenvalue of the corresponding mode. The curve $k_i^+ = 0$ determines the value of DU/DU_{max} at which the peak occurs. We see that as $\bar{U}$ is increased, the position of the peak shifts to smaller DU, i.e., downstream. The theoretically predicted peak positions are shown as vertical dashed lines in Figs. 6 and 8; it is evident that the agreement with the numerical results is excellent. From Fig. 11 we see also that $(DU/DU_{max}, \bar{U}/DU_{max})$ must fall below the $k_i^+ = 0$ curve at large x for the mode to be localized. For Profile 2 (which has $DU(\infty)/DU_{max} = 0.5$), the mode loses its localization for $\bar{U}/DU_{max} > 0.5$, in accord with the numerical results. Also in agreement with the numerical results is the fact that the decay scale downstream of the peak becomes shorter when either $\bar{U}$ or $DU(\infty)$ is decreased. Fig. 11 can also be used to analyze the structure of modes on profiles for which both $\bar{U}$ and DU vary in x.

The anatomy of the local modes is summarized pictorially in Fig. 12a. In a discussion of local *barotropic* instabilities, Merkine and Balgovind (1983) also pointed out the necessity of branch switching, though without the use of a formal WKB approximation. They speculated that the opportunity for branch switching may be provided in some way by the mathematically intricate features of the nonparallel critical line where phase speed ~ equals zonal velocity. However, the generality of our argument leading to the connection between coalescence and absolute instability leads us to suspect that a similarly simple explanation may exist in the barotropic case.

c. *Anatomy of the global modes*

For global modes the appropriate boundary condition is

$$\hat{\psi}_j(-L/2) = \hat{\psi}_j(L/2), \tag{5.19}$$

where L is the period of the domain. The structure of the global modes is much simpler than that of the local modes, as branch switching need not occur. Consider first a solution

$$\hat{\psi}_j = A_j e^{i\int_{L/2}^{x} k dx}, \tag{5.20}$$

in which $k(DU, U, \omega)$ is a particular branch of the dispersion relation; k will be periodic in x because of

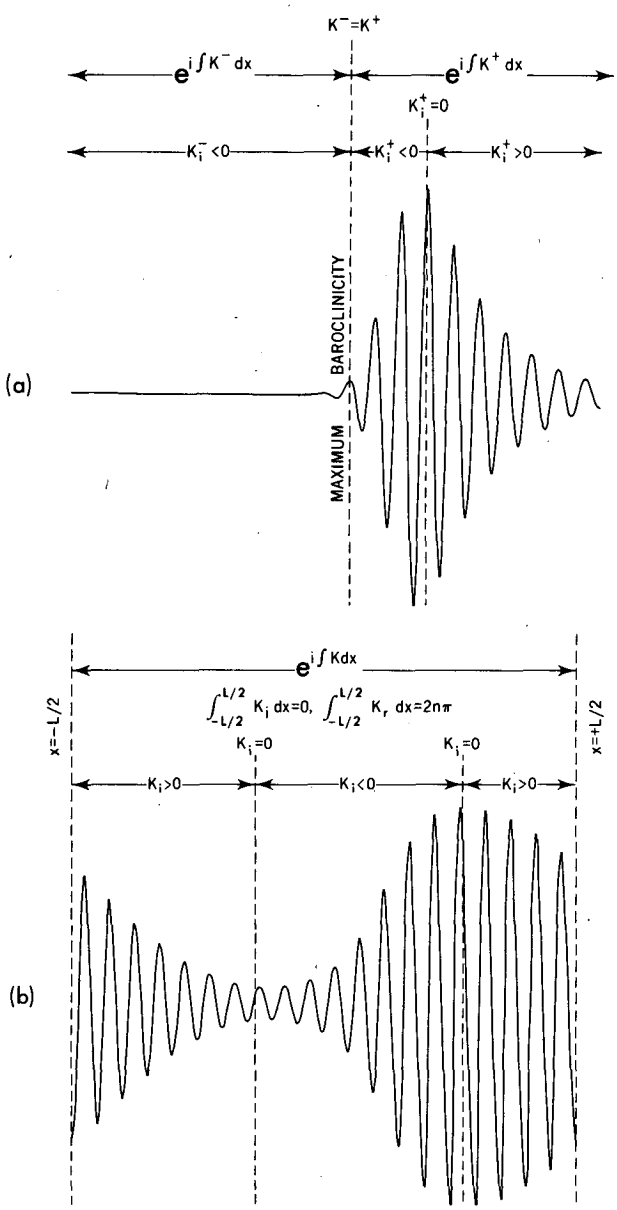

FIG. 12. Summary of structure of (a) local modes and (b) global modes.

the periodicity of DU and $\bar{U}$. Then (5.19) requires that

$$\int_{-L/2}^{L/2} k_i dx = 0, \tag{5.21a}$$

$$\int_{-L/2}^{L/2} k_r dx = 2n\pi, \tag{5.21b}$$

in which n may be any integer. It is easy to show that if the solution were a sum over seven terms of the form (5.20) corresponding to the seven roots of (5.9), then periodicity requires that each term individually must satisfy (5.21). Equation (5.21) determines the eigenvalue ω.

In contrast with the conditions determining ω for local instability, (5.21) is sensitive to the profile of DU and $\bar{U}$ throughout the domain. Eq. (5.21a) implies that k_i must vanish for some ($\bar{U}$, DU) appearing in the flow; this fact leads to a reliable procedure for finding the roots of (5.21), which, for simplicity, we will describe for the case where $\bar{U}$ is constant and DU has a single maximum at $x = 0$. In these circumstances, k_i vanishes at the two points on either side of $x = 0$ where DU attains an as yet unknown value we shall call DU_p. At these points, k has an as yet unknown *real* value which we shall call k_p. Here ω is determined by DU_p and k_p via (5.8). Given ω, k can be found for the rest of the domain using (5.9), and the integrals in (5.21) can be carried out. Our task, then, is to find real values DU_p and k_p such that (5.21) is satisfied.

For each k_p we use Newton's method to find a value DU_p between $DU_{\max}$ and $DU_{\min}$ such that (5.21a) is satisfied. This gives us a family of eigenvalues $[k_p, DU_p(k_p)]$ for which (5.21a) is satisfied. To satisfy (5.21b) we compute

$$\Phi(k_p) = \frac{1}{2\pi}\int_{-L/2}^{L/2} k_r[DU(x), \omega]dx, \tag{5.22}$$

where $\omega = \omega[k_p, DU_p(k_p)]$ on the rhs. By determining where $\Phi(k_p)$ attains integral values, we find the discrete set of k_p for which both (5.21a) and (5.21b) are satisfied; this in turn yields the corresponding discrete set of eigenvalues ω. Note that, by assumption, L is large while k and k_p are order unity quantities. Hence, Φ is a very rapidly varying function of k_p, and only a very small O $(1/L)$ change of k_p is needed to change Φ by unity. In consequence, the eigenvalues will be closely spaced, as was suggested by numerical results described in Section 4.

The above procedure was carried out for Profile 1 and Profile 2 with $\beta = 0.25$ and a range of values of $\bar{U}$. For all unstable modes we found that $k_i < 0$ where $DU > DU_p$, so that the positive value x_p where $DU(x) = DU_p$ is the location of the peak and $-x_p$ is the location of the valley. The general structure is depicted in Fig. 12b. In Fig. 13 we show the global mode growth rate and peak position as a function of $\bar{U}$ for Profile 1 and Profile 2. Only the most unstable mode is plotted. For $\bar{U} = 1$ in the Profile 2 case, the most unstable mode has $\omega = 0.80 + 0.1642i$, which occurs with $\Phi = 12$. The next most unstable mode was found to have $\Phi = 13$ and $\omega = 0.89 + 0.1635i$. Both of these compare reasonably with the numerically determined value $\omega = 0.74 + 0.16i$.

As revealed in Fig. 13, the global mode growth rate is lower for Profile 1 than for Profile 2, in contrast with the behavior of the local mode. This underscores that the global mode is sensitive to the *average* baroclinicity of the domain rather than to the peak baroclinicity. In fact, we can show that

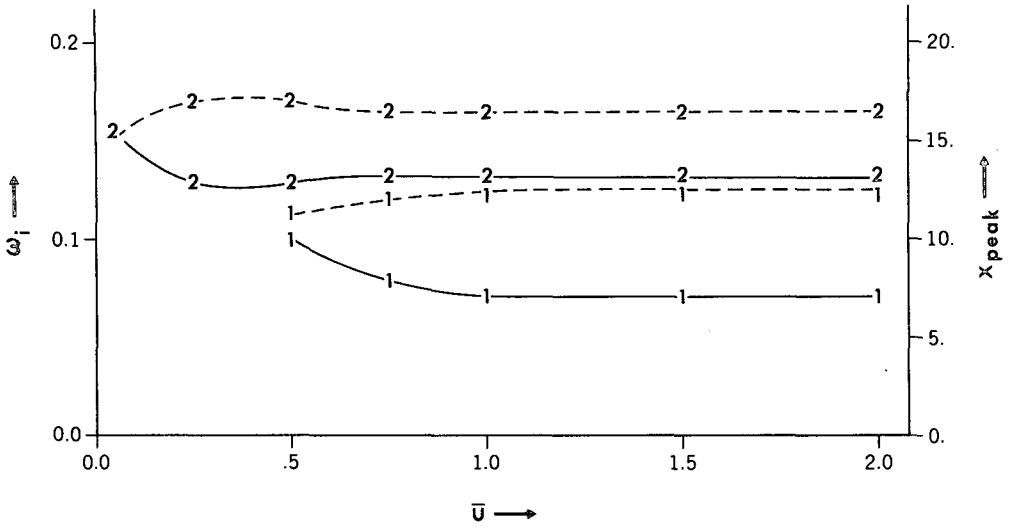

FIG. 13. Theoretical growth rate and peak position for global modes on Profile 1 and Profile 2 as a function of $\bar{U}$. Solid line with ones, growth rate, Profile 1; dashed line with ones, peak position, Profile 1; solid line with twos, growth rate, Profile 2; dashed line with twos, peak position, Profile 2.

when the zonal variations of the basic state are not too strong, the eigenvalue is the same as that for the zonally averaged flow. Let

$$\left.\begin{aligned} DU &= DU_0 + DU_1(x) \\ \bar{U} &= \bar{U}_0 + \bar{U}_1(x) \end{aligned}\right], \tag{5.23}$$

where $DU_1 \ll DU_0$, $U_1 \ll U_0$, U_0 and DU_0 are x-independent, and $\bar{U}_1$ and DU_1 have vanishing zonal means. Next set ω equal to the eigenvalue for the zonal flow (U_0, DU_0) at some real k, so that $k_i(\omega, U_0, DU_0) = 0$. Then, to leading order,

$$k_i(\omega, \bar{U}, DU) = \left(\frac{\partial k_i}{\partial \bar{U}}\bigg|_{\bar{U}_0}\right)\bar{U}_1 + \left(\frac{\partial k_i}{\partial DU}\bigg|_{DU_0}\right)DU_1, \tag{5.24}$$

and (5.21a) is automatically satisfied by virtue of the vanishing zonal means of U_1 and DU_1; hence, ω is also an eigenvalue for the zonally varying flow, to leading order. For Profile 2, the zonal average of DU is 0.5922, and the corresponding growth rate is 0.1493. The growth rate corresponding to the zonally averaged flow in this case is a good estimate of the global mode growth rate, even though the excursions of baroclinicity are not strictly small.

Returning to Fig. 13, we see that the global mode growth rate is relatively insensitive to $\bar{U}$. This is sensible, as the average growth experienced by a wave packet crossing the domain is independent of the time taken to complete a traverse. Also note that the position of peak amplitude occurs downstream of the maximum baroclinicity as for the local modes but that this position is relatively insensitive to $\bar{U}$.

6. Discussion

It is instructive to begin our discussion with an analysis of the results of Frederiksen (1979, 1983) in terms of the concepts developed above. Given the number of simplifying assumptions we have made, this must be regarded as a speculative endeavor, particularly when one considers the difference between absolute instability in the two-layer model and the Charney model (Farrell, 1983). A more quantitative comparison must await further refinements of the local analysis.

In Frederiksen (1979) the stability of an idealized wavenumber 3 pattern in a two-layer fluid was considered. The basic state lower level wind was set identically to zero, so $\bar{U} = 0.5DU$ at each point. Here $DU_{max} \approx 50$ m s^{-1} for the chosen flow, which yields $\beta = 0.2$ if we take $L_d \approx 1000$ km. This value of β is reasonably close to the case $\beta = 0.25$, analyzed in Section 5. The largest value of DU_{min}/DU_{max} that permits localization is given by the intersection of the line $\bar{U} = 0.5DU$ with the curve $k_i = 0$ in Fig. 11; the critical value is thus found to be 0.725. In the idealized flow, $DU_{min}/DU_{max} = 0.66$, which just barely meets the localization criterion. Under these circumstances, the peak of a local mode would occur near the point of minimum DU, which for a wavenumber 3 pattern is 60° of latitude upstream of the next maximum of DU. With $DU_{min}/DU_{max} = 0.66$, the dimensionless downstream decay rate is 0.06, which corresponds to 200° of longitude. Clearly, a local mode cannot exist on the idealized profile because the successive baroclinic zones are too close together. This suggests that the mode found by Frederiksen is a global mode. For a global mode, the peak should

occur roughly midway between DU_{max} and DU_{min}, so as to satisfy (5.21a); consistently, the actual peaks occur about 20° downstream of the points of maximum DU. It was also found that the maximum growth rate for the wavy flow is essentially the same as that for the corresponding zonally averaged flow. This, too, is consistent with the properties of a global mode. As discussed in Section 4 and in Section 5c, global modes are built of wave packets which must traverse regions of both enhanced and depressed baroclinicity, and the net effect of the zonal inhomogeneities on the growth rate is nil when the range of baroclinicity is not too great.

We turn next to the January 1978 monthly mean flow considered in Frederiksen (1983). In order to make use of two-layer results in this case, we estimate DU as the difference between the 500 mb zonal wind in the jet core and the surface wind, and consider the surface wind to be essentially zero. The estimates of DU in the Atlantic and Pacific baroclinic zones are again consistent with the parameter setting $\beta = 0.25$. Also, $DU_{min}/DU_{max} \approx 0.5$ for both zones, where DU_{min} is defined as the first minimum in DU downstream of each region of maximum DU. Estimates based on the nine-winter average data given in Fig. 6a of Blackmon *et al.* (1977) are very similar. Thus, for the realistic winter flow, DU_{min}/DU_{max} is well below the critical value of 0.725 needed for localization. In this case, then, local mode peaks would occur rather upstream of the points of minimum baroclinicity; this is in qualitative agreement with Frederiksen's results. From Fig. 11 the downstream decay rate corresponding to DU_{min} is $k_i = 0.2$, which corresponds to a dimensional e-folding distance of 65° at midlatitudes. The entrance of the Pacific baroclinic zone is more than 180° downstream of the exit of the Atlantic baroclinic zone. Thus, we expect the existence of an isolated Atlantic mode, in accord with Fig. 9a of Frederiksen (1983). By contrast, the entrance of the Atlantic zone is, at best, 90° downstream of the exit of the Pacific zone. There is enough room for the local Pacific mode to decay by perhaps a factor of $1/e$ before the Atlantic baroclinic zone is encountered; at that point k_i becomes negative again, and the mode begins growing in the downstream direction. Because the amplitude has not decayed greatly at the entrance of the Atlantic zone, we expect a prominent secondary maximum to occur in the Atlantic. The resulting structure is in accord with that shown in Frederiksen's Fig. 9b. Frederiksen reports a growth rate of 0.4318 day^{-1} for the most unstable mode on the wavy January flow, as opposed to 0.35 day^{-1} for the corresponding zonally averaged flow. This is also suggestive of a local mode for which the growth rate is sensitive to the maximum baroclinicity rather than the average. In fact, with $DU = 50$ m s^{-1} the dimensional growth rate at $\beta = 0.25$ and $DU = 0.5U$ in the idealized case we have treated is 0.5 day^{-1}, in good agreement with Frederiksen's calculation.

Frederiksen (1983) also considered the instability of the July 1978 monthly mean flow. However, because the July results are dominated by internal baroclinic–barotropic instabilities which are not even qualitatively reproduced by two-layer models, we will not attempt an exegesis of this case.

In interpreting our results, or indeed the results of any eigenvalue calculation, it should be kept in mind that the eigenmodes do not tell the whole story. This is so because it takes time for an initial perturbation to evolve into an eigenmode, and the growth characteristics in the transient stage may differ substantially from those of the eigenmodes. It is thus possible for nonlinear effects to become important before a modal form can be attained, as was discussed by Farrell (1982) in the parallel flow case. In the case we have treated, an initial perturbation localized in a region of high baroclinicity will grow at the local maximum growth rate until the transients have had time to move away; thereafter, the perturbation attains the form of a local eigenmode and the growth rate falls to the lower (and possible vanishing) absolute growth rate. For a baroclinic zone of length 6000 km the local mode setup time would be 2.4 days if the transient peak moved at a speed of 25 m s^{-1}. Under these circumstances it is plausible that the form of a local eignmode would be attained before nonlinearity began to dominate the evolution, provided that the amplitude of the initial perturbation was not too great. On the other hand, the coupling of the Atlantic to the Pacific storm track discussed above requires that a perturbation leaving the Pacific storm track survive long enough to enter the Atlantic baroclinic zone, which would require perhaps two to three days beyond the time needed to set up the Pacific mode. It is not clear whether the lifetime of a baroclinic disturbance can be long enough to permit the coupling. To set up a global mode from a spatially random or localized initial condition would require at least one global traverse time (about 15 days at 25 m s^{-1}); it is thus unlikely that the most unstable global mode would ever appear in the atmosphere. The global modes are only physically relevant when used in superposition to represent the transient evolution of wave packets. The same comment applies to the conventional *zonally homogeneous* stability problem, for which all modes are global modes.

We have seen that the local modes derive their localization from the fact that the part of the initial perturbation left behind in the baroclinic zone grows faster than the part that moves away. This mechanism is a purely linear phenomenon. Nonlinearity will become important first near the region of peak amplitude of the linear mode; if the amplitude saturates there and stops growing, the continued exponential growth of the downstream tail will eventually lead to a substantial increase in the downstream penetration. At this stage, the spatial scale of localization will be determined by nonlinear processes governing the

distances baroclinic disturbances can propagate before they mature and decay. In this connection, it is significant that the observed 300 mb bandpass geopotential height standard deviation shown in Fig. 3b of Blackmon *et al.* (1977) shows considerably less zonal localization than the corresponding result based on linear theory. [Frederiksen (1983) shows only the 900 mb patterns, but states that the patterns at higher levels are very similar.] The situation is entirely analogous to that which arises in connection with the *vertical* penetration of baroclinic disturbances growing on a *zonal* flow. Charney and Pedlosky (1963) have shown that in linear theory, such disturbances decay with height; a similar interpretation to that we have given for horizontal decay could be attached to this result. On the other hand, Simmons and Hoskins (1978) have shown that the perturbation equilibrates first near the ground, whereafter the pattern aloft takes the form of a vertically propagating Rossby wave pulse which extends the depth of penetration. By analogy, we expect a complete understanding of the horizontal distribution of eddy energy and momentum flux in the zonally inhomogeneous case to require consideration of the full nonlinear life cycle of the disturbance.

7. Conclusions

Within the context of a simplified model, we have shown that a zonally varying steady flow can possess two distinct classes of baroclinically unstable eigenmodes, which we have referred to as "local" and "global". Local modes have a peak downstream of the point of maximum baroclinicity of the basic state flow, and decay to zero both downstream and upstream of the peak. The growth rate of a local mode is approximately equal to the absolute growth rate (defined in Section 3) at the point of maximum baroclinicity. This growth rate increases with the maximum baroclinicity obtaining in the flow, and decreases with increasing vertically averaged zonal flow. The latter property contrasts with the conventional local maximum growth rate, which is insensitive to addition of a mean flow. In order for a local mode to exist, two conditions besides absolute instability must be satisifed: 1) the ratio of maximum baroclinicity to the minimum baroclinicity appearing downstream of the maximum must be sufficiently large and 2) successive peaks in baroclinicity must be sufficiently separated to allow the mode associated with each peak to decay appreciably before the next downstream peak is reached. Global modes, on the other hand, require cyclic zonal boundary conditions for their existence. Their growth rate is sensitive to the baroclinicity throughout the domain, and is equal to that of the most unstable mode for the corresponding zonally averaged flow when the zonal range of baroclinicity is not too great. The peak of a global mode also occurs downstream of the point of maximum baroclinicity, but neither the peak position nor the growth rate is very sensitive to the vertical mean flow. The global modes form a near continuum, and owing to the large time required for a single mode to emerge from random initial conditions, it is suggested that they are only physically relevant insofar as they can be used in combination to represent the evolution of transient wave packets. The above results have been established quantitatively both in numerical simulations and via a WKB asymptotic analysis of the model problem.

We have pointed out that even in situations in which a local mode eventually dominates, the transient growth rate occurring during the time required for the modal form to be attained can be considerably greater than the ultimate local mode growth rate. The net transient growth is dependent on the residence time of a transient disturbance in the highly baroclinic zone (roughly the length of the zone divided by the vertical mean flow); for large residence times, nonlinear effects would be likely to set in before the modal form is attained. The scales characterizing the winter Northern Hemisphere baroclinic zones in the Atlantic and Pacific are such that the emergence of local modes is plausible. We have also argued that nonlinear effects may act to delocalize the disturbance in the *zonal* direction, much as they are known to extend the *depth* of baroclinic eddies in the zonally homogeneous case.

A tentative comparison with the results of Frederiksen (1979, 1983) was found to be encouraging, though a precise comparison would require the extension of our results to basic states with continuous vertical and horizontal shear. The nature of the theory, though, offers good possibilities for such a generalization, provided that the main assumption of separation in scales between eddies and the zonal variation of the basic state is retained. While we do not believe that a local analysis along these lines can ever supplant calculations of the sort described by Frederiksen, we suggest that the diagnosis of local absolute growth rate can assist the physical understanding of the connection between the inhomogeneities of a basic state and the preferred regions of synoptic eddy activity associated with that state.

REFERENCES

Blackmon, M. L., J. M. Wallace, N. Lau and S. Mullen, 1977: An observational study of the Northern Hemisphere wintertime circulation. *J. Atmos. Sci.*, **34**, 1040–1053.

Charney, J. G., and J. Pedlosky, 1963: On the trapping of unstable planetary waves in the atmosphere. *J. Geophys. Res.*, **68**, 6441–6442.

Farrell, B., 1982: The initial growth of disturbances in a baroclinically unstable flow. *J. Atmos. Sci.*, **39**, 1663–1686.

——, 1983: Pulse asymptotics of three-dimensional baroclinic waves. *J. Atmos. Sci.*, **40**, 2202–2210.

Frederiksen, J. S., 1978: Instability of planetary waves and zonal flows in two-layer models on a sphere. *Quart. J. Roy. Meteor. Soc.*, **104**, 841–872.

——, 1979: The effect of long planetary waves on the regions of cyclogenesis: Linear theory. *J. Atmos. Sci.*, **36**, 195–204.

——, 1980: Zonal and meridional variations of eddy fluxes induced by long planetary waves. *Quart. J. Roy. Meteor. Soc.*, **106,** 63–84.

——, 1983: Disturbances and eddy fluxes in Northern Hemisphere flows: Instability of three-dimensional January and July flows. *J. Atmos. Sci.*, **40,** 836–855.

Gent, P. R., and H. Leach, 1976: Baroclinic instability in an eccentric annulus. *J. Fluid Mech.*, **77,** 769–788.

Green, J. S. A., 1977: The weather during July 1976: Some dynamical considerations concerning the drought. *Weather,* **32,** 120–128.

Hoskins, B. J., I. N. James and G. H. White, 1983: The shape, propagation and mean-flow interaction of large-scale weather systems. *J. Atmos. Sci.*, **40,** 1595–1612.

Illari, L., and J. C. Marshall, 1983: On the interpretation of eddy fluxes during a blocking episode. *J. Atmos. Sci.*, **40,** 2232–2242.

Lindzen, R. S., B. Farrell and A. J. Rosenthal, 1983: Absolute barotropic instability and monsoon depressions. *J. Atmos. Sci.*, **40,** 1178–1184.

Merkine, L., 1977: Convective and absolute instability of baroclinic eddies. *Geophys. Astrophys. Fluid Dyn.*, **9,** 129–157.

——, and M. Shafranek, 1980: The spatial and temporal evolution of localized unstable baroclinic disturbances. *Geophys. Astrophys. Fluid Dyn.*, **16,** 174–206.

——, and R. Balgovind, 1983: Barotropic instability of weakly non-parallel zonal flows. *Geophys. Astrophys. Fluid Dyn.*, **25,** 157–190.

Niehaus, M. C. W. 1980: Instability of non-zonal baroclinic flows. *J. Atmos. Sci.*, **37,** 1447–1463.

——, 1981: Instability of non-zonal baroclinic flows: Multiple-scale analysis. *J. Atmos. Sci.*, **38,** 974–987.

Pedlosky, J., 1979: *Geophysical Fluid Dynamics.* Springer-Verlag, 312 pp.

Simmons, A. J., and B. Hoskins, 1978: The life cycles of some nonlinear baroclinic waves. *J. Atmos. Sci.*, **35,** 414–432.

——, J. M. Wallace and G. W. Branstator, 1983: Barotropic wave propagation and instability and atmospheric teleconnection patterns. *J. Atmos. Sci.*, **40,** 1363–1392.